

KEK-TH-586

OU-HET-303

YITP-98-57

hep-ph/yymmdd

December 2, 2024

Lepton-Flavor Violation
in the Left-handed Slepton Production
at Future Lepton Colliders

Junji Hisano^(a), Mihoko M. Nojiri^(b), Yasuhiro Shimizu^(a), and
Minoru Tanaka^(c)

(a) Theory Group, KEK, Oho 1-1, Tsukuba, Ibaraki 305-0801, Japan

(b) YITP, Kyoto University, Kyoto 606-8502, Japan

*(c) Department of Physics, Graduate School of Science, Osaka University, Toyonaka,
Osaka 560-0043, Japan*

Abstract

The Super-Kamiokande atmospheric neutrino data suggest existence of the large lepton-flavor violating (LFV) interaction in the higher energy scale. If the minimal supersymmetric standard model is extended to have right-handed neutrinos, the left-handed sleptons in the second and third generations are expected to have the LFV masses in the minimal supergravity scenario. In this article we study the LFV signals in the left-handed slepton production at $\mu^+\mu^-$ colliders and e^+e^- linear colliders (LC's), $\mu^+\mu^-(e^+e^-) \rightarrow \tau\mu + 4\text{jets} + \cancel{E}$ and $\mu^+\mu^-(e^+e^-) \rightarrow \tau\mu l + 2\text{jets} + \cancel{E}$. The main background comes from decay of a tau lepton into a muon in the lepton-flavor conserving slepton pair production. They are significantly reduced by the energy and the impact parameter cuts for the muon. At $\mu^+\mu^-$ colliders (LC's) it may be possible to reach the mixing angle $\sin 2\theta_{\tilde{\nu}} \gtrsim 0.1(0.5)$ and the mass difference $\Delta m_{\tilde{\nu}} \gtrsim 0.1(0.4)$ GeV for the sneutrinos in the second and third generations at the statistical significance of 3σ . Such small mass difference and a mixing angle may be induced radiatively even if the Yukawa coupling constant for the tau neutrino is of the order of 0.1.

1 Introduction

The Super-Kamiokande collaboration has reported evidence that the atmospheric neutrino anomaly is indeed due to neutrino oscillation [1]. This phenomenon is lepton-flavor violating (LFV), and it is the first convincing signature beyond the standard model (SM). From the zenith-angle dependence of ν_e and ν_μ fluxes following neutrino mass square difference and a mixing angle are favored,

$$\begin{aligned}\Delta m_{\nu_\mu \nu_X}^2 &\simeq (5 \times 10^{-4} - 6 \times 10^{-3}) \text{eV}^2, \\ \sin^2 2\theta_{\nu_\mu \nu_X} &> 0.82.\end{aligned}\tag{1}$$

Provided mass hierarchy $m_{\nu_\tau} \gg m_{\nu_\mu} \gg m_{\nu_e}$ it is natural to consider $\nu_X = \nu_\tau$ while the solar neutrino deficit is explained by the MSW [2] or the vacuum oscillation between ν_μ and ν_e . This is also consistent with the result of the CHOOZ experiment [3]. Thus, the atmospheric neutrino anomaly implies a non-vanishing neutrino mass,

$$m_{\nu_\tau} \simeq (0.02 - 0.08) \text{eV}.\tag{2}$$

The simplest model to generate the neutrino masses is the seesaw mechanism [4]. The neutrino mass Eq. (2) leads to the right-handed neutrino masses below $\sim (10^{14} - 10^{15})$ GeV, even if the Yukawa coupling constant of the right-handed neutrino is of the order of 1. This means that a LFV interaction between the second and third generations exists below the gravitational scale ($M_G \sim 10^{18}$ GeV).

The supersymmetric (SUSY) extension of the standard model (MSSM) is also one of the most promising model beyond the SM [5]. It is one of the solutions to the naturalness problem for the Higgs mass. The SUSY breaking masses for sleptons in the MSSM are sensitive to the physics beyond the MSSM if they are originated from the hidden sector in the minimal supergravity (that is, the minimal supergravity scenario). Especially, if the LFV interaction exists below the gravitational scale, the radiative correction generates the LFV masses for sleptons, and this predicts the LFV processes at low energy, $\mu \rightarrow e\gamma$, $\tau \rightarrow \mu\gamma$, and so on [6]. Many studies have been done for them [7][8][9][10][11][12]. The large mixing between ν_μ and ν_τ suggests the large mixing between the left-handed sleptons in the second and third generations ($\tilde{\mu}_L$ and $\tilde{\tau}_L$, and $\tilde{\nu}_\mu$ and $\tilde{\nu}_\tau$) in the minimal supergravity

scenario. One of the predictions is $\tau \rightarrow \mu\gamma$. However, the future experiments may not reach to the expected branching ratio due to the low sensitivity [12].

In this article, we study an alternative way, search for the LFV in the left-handed slepton production at future lepton colliders, such as the e^+e^- linear colliders (LC's) and $\mu^+\mu^-$ colliders. When the left-handed sleptons in the second and third generations have the LFV masses, the signatures are following,

$$\begin{aligned} 1) \quad & e^+e^- (\mu^+\mu^-) \rightarrow \tilde{\nu}\tilde{\nu}^c \text{ or } \tilde{l}^+\tilde{l}^- \rightarrow \tau\mu + 4\text{jets} + \cancel{E}, \\ 2) \quad & e^+e^- (\mu^+\mu^-) \rightarrow \tilde{\nu}\tilde{\nu}^c \rightarrow \tau\mu l + 2\text{jets} + \cancel{E}, \\ 3) \quad & e^+e^- (\mu^+\mu^-) \rightarrow \tilde{l}^+\tilde{l}^- \rightarrow \tau\mu ll + 2\text{jets} + \cancel{E}, \end{aligned} \quad (3)$$

with ($l = e, \mu, \tau$). The jets and additional leptons in the final states come from the decay of the wino-like chargino and neutralino, into which the left-handed sleptons decay dominantly if the decay modes are open. We find that for the one year of the proposed LC ($\mu^+\mu^-$ collider) run, it may be possible to reach the mixing angle $\sin 2\theta_{\tilde{\nu}} \gtrsim 0.5(0.1)$ and the mass difference $\Delta m_{\tilde{\nu}} \gtrsim 0.4(0.1)\text{GeV}$ for the sneutrinos in the second and third generations at the statistical significance of 3σ . Such small mass difference and a mixing angle may be generated radiatively even if the Yukawa coupling constant of the tau neutrino is almost as large as that of the tau lepton at low $\tan\beta$ ($f_{\nu_\tau} \sim 0.1$). We may observe the LFV processes at future colliders if the large mixing of neutrinos originates from the large mixing of the neutrino Yukawa coupling constants.

Searching for these signals has some advantages. First, these processes are at tree level while $\tau \rightarrow \mu\gamma$ is an one-loop process. This means that we do not need so high statistics compared with $\tau \rightarrow \mu\gamma$. Also, even if the sleptons are degenerate in the masses, the cross sections for the signals are suppressed by at most $\Delta m_{\tilde{l}}/\Gamma_{\tilde{l}}$ with the mass difference of the sleptons $\Delta m_{\tilde{l}}$ and the total width $\Gamma_{\tilde{l}}$ [13][14]. This dependence comes from the interference between the real slepton production and the virtual one in the above signals. The decay widths for the left-handed sleptons are about 1GeV. On the other hand, $\tau \rightarrow \mu\gamma$ is strongly suppressed by $\Delta m_{\tilde{l}}/\bar{m}_{\tilde{l}}$ when $\bar{m}_{\tilde{l}}$ is the average of the slepton masses, since only the virtual slepton exchange contributes to it.

Second, these signals are almost free from the SM backgrounds (BG's) since they have two or more jets and two or more leptons with different flavors in the final states

due to the cascade decays of the SUSY particles. It is shown in Ref. [15] that for the electron sneutrino production at LC's, $e e \mu + 2 jets + \cancel{E}$ is BG free. In the previous works [13][14][16][17][18] only the LFV signal in the slepton production sequel to decay into the LSP directly is studied.

Third, in $\mu^+ \mu^-$ colliders the cross section for muon sneutrino production reaches to 1pb, and we may get enough statistics for search and study of the LFV in the sneutrino masses. The sneutrino mass matrix is determined by only the SUSY breaking mass parameters for the left-handed sleptons, while that for the charged sleptons depends on them and the other parameters. Then, we can extract information on the SUSY breaking mass parameters for the left-handed sleptons directly from the signal through the sneutrino production, $\mu^+ \mu^- \rightarrow \tau \mu l + 2 jets + \cancel{E}$.

Contents of this article are following. In the next section, we discuss the origin of the large mixing suggested from the Super-Kamiokande result, and review the radiative generation of the LFV masses for the left-handed sleptons in the seesaw mechanism. In Section 3 the formula of the cross sections for the LFV signals in a case where the left-handed sleptons have the LFV masses, and the signal cross sections are given for a representative parameter set. In Section 4 we discuss the BG's for the signals. The main BG's come from lepton-flavor conserving $\tilde{\nu}_\tau$ or $\tilde{\tau}_L$ pair production, since τ can decay into μ . We show that the cuts on the energy and the impact parameter (IP) are useful to separate the primary muon from the slepton decay and the secondary muon from the tau decay. Also, we show the significance of the signals over the BG's in LC and muon collider experiments. Section 5 is Conclusion and Discussion. Appendices A and B are for our convention for the MSSM Lagrangian. In Appendix C we show the matrix elements for the slepton production and the decay. In Appendix D the three-body decay widths for the charginos and neutralinos are given. In Appendix E we present the formula of the energy and IP distribution for muon from the tau decay.

2 Radiative generation of the LFV slepton masses in the seesaw mechanism

In this section, we will discuss the origin of the large mixing angle for the atmospheric neutrino observation, and explain the radiative generation of the LFV masses for the left-handed sleptons. Assuming that the atmospheric neutrino observation comes from the oscillation between ν_μ and ν_τ , the Super-Kamiokande result for the atmospheric neutrino may mean existence of the large mixing between the second and third generations in the Yukawa coupling for the neutrinos. In this case, the mixing generates the LFV masses in $\tilde{\tau}_L$ - $\tilde{\mu}_L$ and $\tilde{\nu}_\tau$ - $\tilde{\nu}_\mu$ radiatively in the minimal supergravity scenario,

The MSSM with the right-handed neutrinos (MSSMR) is the simplest supersymmetric model to explain the neutrino masses. The superpotential of the lepton sector is given as

$$W_{\text{MSSM}+\nu_R} = f_{\nu_i} H_2 N_i^c L_i + f_{l_i} U_{Dij}^\dagger H_1 E_i^c L_j + \frac{1}{2} M_{ij} N_i^c N_j^c, \quad (4)$$

where L is left-handed leptons, and N^c and E^c are right-handed neutrinos and charged leptons.¹ H_1 and H_2 are the Higgs doublets in the MSSM. Here, i and j are generation indices. A unitary matrix U_D is similar to the Cabibbo-Kobayashi-Maskawa (CKM) matrix in the quark sector. After the right-handed neutrinos are integrated out, the mass matrix for the left-handed neutrinos is given as

$$\begin{aligned} (m_{\nu_L})_{ij} &= m_{\nu_i D} \left[M^{-1} \right]_{ij} m_{\nu_j D} \\ &\equiv U_{Mik}^T m_{\nu_k} U_{Mkj}, \end{aligned} \quad (5)$$

where U_M is a unitary matrix and

$$m_{\nu_i D} = f_{\nu_i} v \sin \beta / \sqrt{2}, \quad (6)$$

where $\langle H_2 \rangle = (0, v \sin \beta / \sqrt{2})^T$ with $v \simeq 246 \text{ GeV}$. We assume $m_{\nu_\tau} \gg m_{\nu_\mu} \gg m_{\nu_e}$ to explain the atmospheric and the solar neutrino observations naturally, and we consider only the tau and muon neutrino masses here.² Also, we assume that the Yukawa coupling

¹ We represent superfields in capital letters, and the components in small letters.

² We keep three generation indices in our numerical calculation though we neglect indices for the first generation here.

and the Majorana masses for the right-handed neutrinos are real for simplicity. We parameterize two unitary matrices as

$$U_D = \begin{pmatrix} \cos \theta_D & \sin \theta_D \\ -\sin \theta_D & \cos \theta_D \end{pmatrix}, \quad U_M = \begin{pmatrix} \cos \theta_M & \sin \theta_M \\ -\sin \theta_M & \cos \theta_M \end{pmatrix}. \quad (7)$$

The angle between ν_μ and ν_τ is related to θ_D and θ_M by

$$\theta_{\nu_\mu \nu_\tau} = \theta_D + \theta_M. \quad (8)$$

However, in order to derive large θ_M we need to fine-tune the independent Yukawa coupling constants and the mass parameters as explained below. The neutrino mass matrix (m_{ν_L}) in the second and third generations is written explicitly by

$$(m_{\nu_L}) = \frac{1}{1 - \frac{M_{\mu\tau}^2}{M_{\mu\mu} M_{\tau\tau}}} \begin{pmatrix} \frac{m_{\nu_\mu D}^2}{M_{\mu\mu}} & -\frac{m_{\nu_\mu D} m_{\nu_\tau D}}{M_{\mu\tau}} \frac{M_{\mu\tau}^2}{M_{\mu\mu} M_{\tau\tau}} \\ -\frac{m_{\nu_\mu D} m_{\nu_\tau D}}{M_{\mu\tau}} \frac{M_{\mu\tau}^2}{M_{\mu\mu} M_{\tau\tau}} & \frac{m_{\nu_\tau D}^2}{M_{\tau\tau}} \end{pmatrix}. \quad (9)$$

Then, if the following relations are imposed, the neutrino mass hierarchy $m_{\nu_\tau} \gg m_{\nu_\mu}$ and $\theta_M \simeq \pi/4$ can be derived,

$$\frac{m_{\nu_\tau D}^2}{M_{\tau\tau}} \simeq \frac{m_{\nu_\mu D}^2}{M_{\mu\mu}} \simeq \frac{m_{\nu_\mu D} m_{\nu_\tau D}}{M_{\mu\tau}}. \quad (10)$$

We need some mechanism to explain the relation among the independent coupling constants and masses. Also, if $m_{\nu_\tau D} \gg m_{\nu_\mu D}$, similar to the quark sector, the mixing angle θ_M is suppressed as

$$\tan 2\theta_M \simeq -2 \left(\frac{m_{\nu_\mu D}}{m_{\nu_\tau D}} \right) \left(\frac{M_{\mu\tau}}{M_{\mu\mu}} \right), \quad (11)$$

as far as the Majorana masses for right-handed neutrinos do not have stringent hierarchical structure as Eq. (10). Therefore, in the following discussion we assume that the large mixing angle between ν_τ and ν_μ comes from θ_D .

In the minimal supergravity scenario the LFV masses for the left-handed sleptons may be induced radiatively if the MSSM is extended to have the right-handed neutrinos [10]. The SUSY breaking part of the lepton sector in the MSSMR is given as

$$\begin{aligned} -\mathcal{L}_{soft} = & (m_{\tilde{L}}^2)_i^j \tilde{l}_L^i \tilde{l}_{Lj} + (m_{\tilde{e}}^2)_j^i \tilde{e}_{Ri}^* \tilde{e}_R^j + (m_{\tilde{\nu}}^2)_j^i \tilde{\nu}_{Ri}^* \tilde{\nu}_R^j \\ & + (A_l^{ij} h_1 \tilde{e}_{Ri}^* \tilde{l}_{Lj} + A_\nu^{ij} h_2 \tilde{\nu}_{Ri}^* \tilde{l}_{Lj} + \frac{1}{2} b_{ij} \tilde{\nu}_{Ri}^* \tilde{\nu}_{Rj}^* + h.c.), \end{aligned} \quad (12)$$

where terms in the first line are the SUSY breaking masses for the left-handed and the right-handed sleptons, and those in the second lines are the SUSY breaking terms associated with the supersymmetric Yukawa couplings and masses. In the minimal supergravity scenario the SUSY breaking parameters at the gravitational scale (M_G) are

$$(m_L^2)_i^j = (m_{\tilde{e}}^2)_i^j = (m_{\tilde{\nu}}^2)_i^j = m_0^2 \delta_i^j, \quad (13)$$

$$A_\nu^{ij} = f_\nu^{ij} a_0, \quad A_l^{ij} = f_l^{ij} a_0, \quad (14)$$

$$b_{ij} = M_{ij} b_0. \quad (15)$$

These relations for the SUSY breaking parameters are unstable for the radiative correction, and the LFV masses for the left-handed sleptons are generated by the LFV Yukawa interaction for the neutrinos. Here, we assume that the Yukawa coupling constants for right-handed neutrinos in Eq. (4) have hierarchical structure ($f_{\nu_\tau} \gg f_{\nu_\mu} \gg f_{\nu_e}$). In this case, the Yukawa interaction reduces only $(m_L^2)_\tau^\tau$ at the right-handed neutrino scale (M_{ν_R}) as

$$(m_L^2) = \begin{pmatrix} \bar{m}^2 & \\ & \bar{m}^2 - \Delta m^2 \end{pmatrix}. \quad (16)$$

We consider only the left-handed slepton masses in the second and third generations here, again. Here \bar{m}^2 is evaluated by one-loop level renormalization group (RG) equations as

$$\bar{m}^2 = m_0^2 + \frac{3}{2} M_2^2(M_{\nu_R}) \left(\left(\frac{g_2^2(M_G)}{g_2^2(M_{\nu_R})} \right)^2 - 1 \right) + \frac{1}{22} M_1^2(M_{\nu_R}) \left(\left(\frac{g_Y^2(M_G)}{g_Y^2(M_{\nu_R})} \right)^2 - 1 \right) \quad (17)$$

where M_2 and M_1 are the wino and bino masses. Here \bar{m}^2 becomes larger than m_0^2 due to the gauge interactions. Assuming the GUT relation for the gaugino masses, $\bar{m}^2 - m_0^2$ is almost as large as square of the wino mass at the weak scale. Though we need numerical calculation in order to evaluate Δm^2 by the RG equations, it becomes

$$\Delta m^2 = \frac{1}{4\pi^2} f_{\nu_\tau}^2 (3 + a_0^2) m_0^2 \log \frac{M_G}{M_{\nu_R}}, \quad (18)$$

at the logarithmic approximation of one-loop level. In Eq. (18) we ignore the radiative correction by the Yukawa couplings for charged leptons. The mass-square difference Δm^2 is proportional to m_0^2 .

Below the right-handed neutrino scale, it is convenient to take basis of lepton where the Yukawa coupling constants for charged leptons are diagonal,

$$W_{\text{MSSM}} = f_{l_i} H_1 E_i^c L_i + \frac{2m_{\nu_k}}{v^2 \sin^2 \beta} (U_M U_D)_{ki} (U_M U_D)_{kj} L_i L_j H_2 H_2, \quad (19)$$

so that the supersymmetric Yukawa couplings are lepton-flavor conserving. In this basis, (m_L^2) becomes

$$(m_L^2) = U_D^\dagger \begin{pmatrix} \bar{m}^2 & \\ & \bar{m}^2 - \Delta m^2 \end{pmatrix} U_D. \quad (20)$$

The LFV off-diagonal terms in (m_L^2) are controlled by U_D and $\Delta m^2/m^2$. It is important that if the m_0 is comparable to or smaller than M_2 and M_1 (this means that the left-handed slepton masses are larger than the wino and bino masses), the LFV in the left-handed slepton mass matrix is suppressed.

Similarly, the radiative correction generates the off-diagonal components of A_l . Since A_l is proportional to the Yukawa coupling constants, it is not relevant to our following discussion.

We parameterize sneutrino mass matrix by $\sin 2\theta_{\tilde{\nu}}$ and mass splitting between two non-electron sneutrinos $\Delta m_{\tilde{\nu}}$ as

$$(m_{\tilde{\nu}}) = \begin{pmatrix} \cos \theta_{\tilde{\nu}} & -\sin \theta_{\tilde{\nu}} \\ \sin \theta_{\tilde{\nu}} & \cos \theta_{\tilde{\nu}} \end{pmatrix} \begin{pmatrix} \bar{m}_{\tilde{\nu}}^2 & 0 \\ 0 & (\bar{m}_{\tilde{\nu}} - \Delta m_{\tilde{\nu}})^2 \end{pmatrix} \begin{pmatrix} \cos \theta_{\tilde{\nu}} & \sin \theta_{\tilde{\nu}} \\ -\sin \theta_{\tilde{\nu}} & \cos \theta_{\tilde{\nu}} \end{pmatrix}. \quad (21)$$

They are shown as functions of the right-handed neutrino mass scale in Fig. (1). This is derived by solving the RG equations at one-loop level numerically.³ Here, we take $m_{\nu_\tau}^2 = 0.005 \text{ eV}^2$, $\theta_D = \pi/4$, $\bar{m}_{\tilde{\nu}} = 180 \text{ GeV}$, and $\tan \beta = 3, 10, 30$. For simplicity, the gaugino masses in the MSSM are given by the GUT relation, and the lightest chargino mass is fixed to 100 GeV. If f_τ is negligible, $\Delta m_{\tilde{\nu}}$ depends on $f_{\nu_\tau}^2$ (or the right-handed neutrino scale, $M_{\nu_R} = f_{\nu_\tau}^2 v^2 \sin^2 \beta / 2m_{\nu_\tau}$) and $\theta_{\tilde{\nu}}$ is almost as large as θ_D . On the other hand, when f_τ is larger than f_{ν_τ} , $\theta_{\tilde{\nu}}$ becomes smaller since $\Delta m_{\tilde{\nu}}$ is determined by f_τ , not f_{ν_τ} . Notice that the magnitude of the LFV processes depends on $\sin 2\theta_{\tilde{\nu}} \Delta m_{\tilde{\nu}}$. In both of the region $\sin 2\theta_{\tilde{\nu}} \Delta m_{\tilde{\nu}}$ is almost proportional to $f_{\nu_\tau}^2$ (or M_{ν_R}), and it is not so sensitive to f_τ (or $\tan \beta$). For $M_{\nu_R} \gtrsim 10^{12} \text{ GeV}$ (which corresponds to $f_{\nu_\tau} \gtrsim f_\tau$ and $\tan \beta \geq 3$) we

³ Detailed formulae are given in Ref. [12].

can see $\sin 2\theta \Delta m_{\tilde{\nu}} \gtrsim 0.1 \text{GeV}$ in the plot. This region may be accessible in future lepton colliders as we will show later.

In Fig. (2) the branching ratio of $\tau \rightarrow \mu\gamma$ in this model is shown. The parameters in this figure are the same as in Fig. (1). At large $\tan\beta$ the branching ratio of $\tau \rightarrow \mu\gamma$ is enhanced, and the line for $\tan\beta = 30$ can reach to the present experimental bound. This is because the matrix element of $\tau \rightarrow \mu\gamma$ is almost proportional to $\tan\beta$ due to the dipole structure [12]. At the B factories in KEK or SLAC the branching ratio of $\tau \rightarrow \mu\gamma$ may be probed at the level of $10^{-(7-8)}$. However, they are not sensitive enough to probe the LFV masses for sleptons in low $\tan\beta$ or small f_{ν_τ} . It is important to search for the LFV by direct production of the left-handed slepton in future colliders.

3 Cross Sections for the LFV processes in lepton collisions

In this section we present the formula for the cross sections of the LFV processes induced by the productions of the left-handed sleptons in the second and third generations, and show the expected cross sections of the LFV events.

The characteristic LFV signals are different in SUSY particle mass spectrum. In this article we take the SUSY particle mass spectrum expected in the minimal supergravity scenario. In the scenario it is expected that the LSP is the bino-like neutralino ($\tilde{\chi}_1^0$), and that the second lightest neutralino ($\tilde{\chi}_2^0$) and the lightest chargino ($\tilde{\chi}_1^-$) are wino-like. The LFV signals depend on whether the left-handed sleptons are heavier or lighter than the wino-like chargino and neutralino.

- *Case. (I):* $m_{\tilde{l}_L}, m_{\tilde{\nu}} > m_{\tilde{\chi}_1^-}, m_{\tilde{\chi}_2^0}$

In this case the left-handed sleptons are heavy enough to decay into two-bodies, the wino-like chargino or neutralino and lepton. The signals are $\tau\mu + 4\text{jets} + \cancel{E}$, $\tau\mu l + 2\text{jets} + \cancel{E}$, and $\tau\mu ll + 2\text{jets} + \cancel{E}$ ($l = e, \mu, \tau$), where the missing energy \cancel{E} comes from the LSP's. The main standard model BG comes from the $Z^0W^+W^-$ production process, and the BG cross section is small. The significance of the signal for the BG's may be large if the sleptons have the sizable LFV masses.

- *Case. (II):* $m_{\tilde{l}_L}, m_{\tilde{\nu}} < m_{\tilde{\chi}_1^-}, m_{\tilde{\chi}_2^0}$

The left-handed sleptons decay dominantly into the LSP. The signal is $\tau\mu+ \not{E}$, which comes from the charged slepton pair production. The main SM background comes from the W boson pair production, which reaches to at least several fb in LC's even after the cuts. Then, it is hard to get significant signal over the background in LC's. We will need efforts on reducing the background in order to study this case in LC's. Also, in our model the LFV tends to be suppressed since the gaugino masses at the gravitational scale are larger than m_0 to realize this mass spectrum. Muon colliders may give a chance to study the LFV even in this case since the left-handed smuon pair production cross section may reach to 100fb due to t -channel neutralino exchange. In this article we do not study this case further since in the MSSM and the minimal supergravity scenario there is no region for $m_{\tilde{l}_L}, m_{\tilde{\nu}} < m_{\tilde{\chi}_1^-}, m_{\tilde{\chi}_2^0} < 250\text{GeV}$ and $\tan\beta \lesssim 10$, allowed by the experimental constraints.⁴

Let us present formula for the cross section of $\tau^+\mu^- + \tilde{\chi}_A^-\tilde{\chi}_B^+$ ($A, B = 1, 2$) through the sneutrino pair production in lepton collisions with the center-of-mass energy \sqrt{s} . The subsequent decays of charginos lead to the signals $\tau^+\mu^- + 4\text{jets} + \not{E}$ and so on. The amplitude of this process is given as [14]

$$\begin{aligned} \mathcal{M} &= \sum_{X,Y} \mathcal{M}_{XY}(k^2, \bar{k}^2) \\ &\times \frac{i}{k^2 - m_{\tilde{\nu}_X}^2 + im_{\tilde{\nu}_X}\Gamma_{\tilde{\nu}_X}} \mathcal{M}_{XB\mu}(k^2) \times \frac{i}{\bar{k}^2 - m_{\tilde{\nu}_Y}^2 + im_{\tilde{\nu}_Y}\Gamma_{\tilde{\nu}_Y}} \mathcal{M}_{YA\tau}^\dagger(\bar{k}^2), \end{aligned} \quad (22)$$

where X and Y are indices for the mass eigenstates of sneutrino. The momenta k and \bar{k} are for the sneutrino and the anti-sneutrino. Here, \mathcal{M}_{XY} and \mathcal{M}_{XAi} are amplitudes for production of the X -th and the Y -th off-shell sneutrinos and that for the X -th off-shell sneutrino decay into A -th chargino and i -th lepton. The explicit formulae are given in Appendix C.⁵ From this equation, we get the cross section as

$$\begin{aligned} \sigma &= \int A_{XX'}(k^2) dk^2 \int A_{YY'}(\bar{k}^2) d\bar{k}^2 \\ &\times \sum_{XYX'Y'} \sigma_{XYX'Y'}(k^2, \bar{k}^2) \times \text{Br}_{XX'B\mu}(k^2) \times \text{Br}_{YY'A\tau}(\bar{k}^2). \end{aligned} \quad (23)$$

⁴ We include a constraint from $b \rightarrow s\gamma$ which excludes the large region for $\mu < 0$ [19].

⁵ Here, we omit the indices for the helicities of the initial beams while we show them explicitly in Appendix C.

Here the off-shell sneutrino pair production cross section ($\sigma_{XYX'Y'}(k^2, \bar{k}^2)$) and the branching ratio for off-shell sneutrino decay to the A -th chargino ($\text{Br}_{XYAi}(k^2)$) are

$$\sigma_{XYX'Y'}(k^2, \bar{k}^2) \equiv \int \frac{1}{2s} \mathcal{M}_{XY}(k^2, \bar{k}^2) \mathcal{M}_{X'Y'}^\dagger(k^2, \bar{k}^2) d\Omega_2, \quad (24)$$

$$\text{Br}_{XYAi}(k^2) \equiv \int \frac{1}{2[m\Gamma]_{\tilde{\nu}_X \tilde{\nu}_Y}} \mathcal{M}_{XAi}(k^2) \mathcal{M}_{YAi}^\dagger(k^2) d\Omega_2, \quad (25)$$

where $[m\Gamma]_{XY} = (m_{\tilde{\nu}_X} \Gamma_{\tilde{\nu}_X} + m_{\tilde{\nu}_Y} \Gamma_{\tilde{\nu}_Y})/2$, and $d\Omega_2$ is the two-body phase space integral. The function of the momentum for the sneutrino $A_{XY}(k^2)$ is

$$A_{XY}(k^2) \equiv \frac{1}{2\pi} \frac{2[m\Gamma]_{XY}}{(k^2 - m_{\tilde{\nu}_X}^2 + im_{\tilde{\nu}_X} \Gamma_{\tilde{\nu}_X})(k^2 - m_{\tilde{\nu}_Y}^2 - im_{\tilde{\nu}_Y} \Gamma_{\tilde{\nu}_Y})}. \quad (26)$$

For numerical calculations, we take only singular parts in this function as

$$A_{XY}(k^2) = \frac{1}{1 + ix_{XY}^{(\tilde{\nu})}} \frac{\delta(k^2 - m_{\tilde{\nu}_X}^2) + \delta(k^2 - m_{\tilde{\nu}_Y}^2)}{2}, \quad (27)$$

where

$$x_{XY}^{(\tilde{\nu})} \equiv \frac{m_{\tilde{\nu}_X}^2 - m_{\tilde{\nu}_Y}^2}{2[m\Gamma]_{XY}}. \quad (28)$$

This function gives correct cross section in the interference region $m_{\tilde{\nu}_X}^2 - m_{\tilde{\nu}_Y}^2 \lesssim 2[m\Gamma]_{XY}$ and the decoherent region $m_{\tilde{\nu}_X}^2 - m_{\tilde{\nu}_Y}^2 \gg 2[m\Gamma]_{XY}$. In order to evaluate the cross section in the intermediate region, we have to calculate the full one-loop correction to this process. However, that is out of scope of our paper.

By repeating the above procedure, we can get the cross sections for $\tau^+ \mu^- + \tilde{\chi}_A^0 \tilde{\chi}_B^0$ ($A, B = 1 - 4$) through the charged slepton pair production. Finally, we need to multiply the branching ratios of charginos and neutralinos to the cross sections in order to get the cross sections for the LFV signals, such as $\tau^+ \mu^- + 4\text{jets} + \cancel{E}$ and so on. We present the formula for the decay widths of charginos and neutralinos in Appendix D.

Now, we present the signal cross sections of the signals at LC's and $\mu^+ \mu^-$ colliders. First, we discuss them in LC's. In Fig. (3) we present the cross section of $\tau^+ \mu^- + \tilde{\chi}_1^- \tilde{\chi}_1^+$ induced by the sneutrino pair production and that of $\tau^+ \mu^- + \tilde{\chi}_2^0 \tilde{\chi}_2^0$ induced by the charged slepton pair production. The horizontal line is the mass splitting between two non-electron sneutrinos ($\Delta m_{\tilde{\nu}}$) and the vertical line is the mixing angle ($\sin 2\theta_{\tilde{\nu}}$). Here, we take the center-of-mass energy 500GeV, the heaviest sneutrino (charged slepton) mass

180(194) GeV, the lightest chargino mass 100GeV and $\tan\beta = 3$. For simplicity, we assume only the MSSM here, and the other SUSY particle masses are determined by the minimal supergravity scenario with the GUT relation for the gaugino masses and the radiative breaking condition of $SU(2)_L \times U(1)_Y$ with the Higgsino mass (μ) positive. For this sample parameter set the wino-like neutralino and the left-handed smuon masses are given in Table (1). Also, in Tables (2,3) the charged slepton and the sneutrino pair production cross sections in the LC and the branching ratios in the limit of zero flavor mixing. In order to obtain the signal cross sections for $\tau^+\mu^- + 4\text{jets} + \cancel{E}$ and so on, the branching ratios of the chargino and the neutralino should be known precisely. Since they depend on details of the SUSY breaking mass spectrum, they should be determined experimentally. We present the branching ratios of the wino-like chargino and neutralino in the above assumption in Table (4).

The widths of sleptons are about 1.2 GeV. The signal cross sections are not strongly suppressed if the mass difference $\Delta m_{\tilde{\nu}} \gtrsim 1$ GeV as can be seen from the plots. Therefore it may be possible to search for the LFV experimentally even if the mass difference $\Delta m_{\tilde{\nu}} \simeq 1$ GeV.

In the figure, the cross sections of $\tau^+\mu^- + \tilde{\chi}_1^-\tilde{\chi}_1^+$ and $\tau^+\mu^- + \tilde{\chi}_2^0\tilde{\chi}_2^0$ are comparable. The reason can be understood from the charged slepton and sneutrino pair production cross sections in e^+e^- collisions and the branching ratios in the limit of zero flavor mixing in Tables (2,3). The production cross sections for $\tilde{\mu}_L$ and $\tilde{\tau}_L$ are larger than those for $\tilde{\nu}_\mu$ and $\tilde{\nu}_\tau$ since $\tilde{\mu}_L$ and $\tilde{\tau}_L$ have QED charges. On the other hand, since $\tilde{\chi}_1^-$ and $\tilde{\chi}_2^0$ are wino-like, the left-handed sleptons decay mostly to $\tilde{\chi}_1^-$ and $\tilde{\chi}_2^0$, and $Br(\tilde{f} \rightarrow f'\tilde{\chi}^\pm)$ is larger than $Br(\tilde{f} \rightarrow f\tilde{\chi}_2^0)$ (see Table (3)).⁶ Then, the cross section for $\tau^+\tau^-(\mu^+\mu^-) + \tilde{\chi}_1^-\tilde{\chi}_1^+$ is comparable to that for $\tau^+\tau^-(\mu^+\mu^-) + \tilde{\chi}_2^0\tilde{\chi}_2^0$ in the limit of zero flavor mixing. When $\tilde{\mu}_L$ and $\tilde{\tau}_L$, $\tilde{\nu}_\mu$ and $\tilde{\nu}_\tau$ have sizable mass difference, the cross section for $\tau^+\mu^- + \tilde{\chi}_1^-\tilde{\chi}_1^+$ from the sneutrino production may reach to 2.8fb, and that for $\tau^+\mu^- + \tilde{\chi}_2^0\tilde{\chi}_2^0$ does to 2.3fb at $\tan\beta = 3$. Then, from Table (4), the cross sections for the signals are given approximately

⁶ In pure wino limit $Br(\tilde{f} \rightarrow f'\tilde{\chi}^\pm) : Br(\tilde{f} \rightarrow f\tilde{\chi}_2^0) \sim 2 : 1$. However, in Table (5) the left-handed charged slepton decay into $\tilde{\chi}_1^0(\tilde{\chi}_2^0)$ is suppressed (enhanced) while the sneutrino decay into $\tilde{\chi}_1^0(\tilde{\chi}_2^0)$ is enhanced (suppressed). This comes from interference between wino- and bino-components in the neutralinos.

as

$$\begin{aligned}
\sigma(\tau^+ \mu^- + 4\text{jets} + \cancel{E}) &\simeq 2\chi_{\tilde{\nu}}(3 - 4\chi_{\tilde{\nu}}) \sin^2 2\theta_{\tilde{\nu}} \times 1.2\text{fb}, \\
\sigma(\tau^+ \mu^- l^{\pm} + 2\text{jets} + \cancel{E}) &\simeq 2\chi_{\tilde{\nu}}(3 - 4\chi_{\tilde{\nu}}) \sin^2 2\theta_{\tilde{\nu}} \times 0.22\text{fb}, \\
\sigma(\tau^+ \mu^- l^+ l^- + 2\text{jets} + \cancel{E}) &\simeq 2\chi_{\tilde{\nu}}(3 - 4\chi_{\tilde{\nu}}) \sin^2 2\theta_{\tilde{\nu}} \times 0.15\text{fb},
\end{aligned} \tag{29}$$

where $\chi_{\tilde{\nu}}$ is given as

$$\chi_{\tilde{\nu}} \equiv \frac{(x_{12}^{(\tilde{\nu})})^2}{2(1 + (x_{12}^{(\tilde{\nu})})^2)}. \tag{30}$$

Next, in Fig. (4) we show the cross sections of $\tau^+ \mu^- + \tilde{\chi}_1^- \tilde{\chi}_1^+$ and $\tau^+ \mu^- + \tilde{\chi}_2^0 \tilde{\chi}_2^0$ when $\tan \beta = 10$. The other parameters are the same as in Fig. (3). The cross section of $\tau^+ \mu^- + \tilde{\chi}_2^0 \tilde{\chi}_2^0$ induced by the charged slepton pair production is drastically changed compared to that for $\tan \beta = 3$, while that of $\tau^+ \mu^- + \tilde{\chi}_1^- \tilde{\chi}_1^+$ induced by the sneutrino pair production is not so.

The nontrivial dependence on $\Delta m_{\tilde{\nu}}$ can be explained by the left-right mixing term of the stau's. The charged slepton mass matrix among $\tilde{\mu}_L$, $\tilde{\tau}_L$, and $\tilde{\tau}_R$ is given by

$$\begin{pmatrix} m_{L22}^2 & m_{L23}^2 & 0 \\ m_{L32}^2 & m_{L33}^2 & m_{LR33}^2 \\ 0 & m_{LR33}^2 & m_{R33}^2 \end{pmatrix}, \tag{31}$$

where m_{LR33}^2 is ignored. Each component is given in Appendix B. As explained in Section 2, $m_{L22}^2 \gtrsim m_{L33}^2 \gtrsim m_{R33}^2$ is expected in the minimal supergravity scenario, as far as the strong Yukawa coupling for neutrino does not reduce m_{L33}^2 below m_{R33}^2 . After diagonalizing the submatrix for the left-handed and right-handed stau's, this mass matrix becomes

$$\begin{pmatrix} m_{L22}^2 & m_{L23}^2 \cos \theta_{\tilde{\tau}} & -m_{L23}^2 \sin \theta_{\tilde{\tau}} \\ m_{L23}^2 \cos \theta_{\tilde{\tau}} & m_{\tilde{\tau}_2}^2 & 0 \\ -m_{L23}^2 \sin \theta_{\tilde{\tau}} & 0 & m_{\tilde{\tau}_1}^2 \end{pmatrix}, \tag{32}$$

where $m_{\tilde{\tau}_1}$ and $m_{\tilde{\tau}_2}$ are masses of the stau's and $\theta_{\tilde{\tau}}$ is the mixing angle. They are given as

$$\begin{aligned}
m_{\tilde{\tau}_{1/2}}^2 &= \frac{1}{2} \left(m_{L33}^2 + m_{R33}^2 \mp \sqrt{(m_{L33}^2 - m_{R33}^2)^2 + 4(m_{LR33}^2)^2} \right), \\
\tan 2\theta_{\tilde{\tau}} &= \frac{2m_{LR33}^2}{m_{L33}^2 - m_{R33}^2}.
\end{aligned} \tag{33}$$

When $(m_{L33}^2 - m_{R33}^2)$, which is almost as large as square of the wino mass in the minimal supergravity scenario, is larger than $|m_{LR33}^2|$, the stau masses are given as

$$m_{\tilde{\tau}_{1/2}}^2 = m_{R33/L33}^2 \mp \frac{(m_{LR33}^2)^2}{m_{L33}^2 - m_{R33}^2}. \quad (34)$$

If the left-right mixing for stau's (m_{LR33}^2) is negligible, $\tilde{\tau}_2$ is lighter than $\tilde{\mu}_L$ with finite $\Delta m_{\tilde{\nu}}$. However, when the Higgsino mass or $\tan\beta$ is larger, $|(m_{LR33}^2)|$ is non-negligible, and $\tilde{\tau}_2$ is larger. If $\tilde{\tau}_2$ becomes more degenerate in the masses with $\tilde{\mu}_L$, the mixing angle is enhanced. The cross section is maximum when $m_{L22}^2 - m_{L33}^2 \simeq (m_{LR33}^2)^2 / (m_{L33}^2 - m_{R33}^2)$, which corresponds to $\Delta m_{\tilde{\nu}} \simeq 4$ GeV in Fig. (4). If the Higgsino mass or $\tan\beta$ is much larger and $|m_{L33}^2 - m_{R33}^2|$ is smaller than $|m_{LR33}^2|$, the stau masses become

$$m_{\tilde{\tau}_{1/2}}^2 = \frac{1}{2}(m_{L33}^2 + m_{R33}^2) \mp |m_{LR33}^2|. \quad (35)$$

In this case degeneracy between masses of $\tilde{\tau}_2$ and $\tilde{\mu}_L$ is more accidental, and usually the mixing is reduced effectively [18]. This kind of behavior does not exist in the sneutrino production since the right-handed partners for neutrino decouple at low energy. We can extract directly the information on the LFV in the SUSY breaking mass terms for the left-handed sleptons by studying the signal $\tau\mu l + 2jet + \cancel{E}$ induced by sneutrino production.

Finally, we discuss the cross section for the signal at $\mu^+\mu^-$ colliders. The production cross sections for left-handed sleptons in the second generation are much larger than the others due to t -channel exchanges of charginos or neutralinos. In Table (5) we show the production cross sections for slepton at $\mu^+\mu^-$ colliders are shown in the limit of zero flavor mixing. Here, we take the sample parameter set for $\tan\beta = 3$ in Table (1). The $\tilde{\nu}_\mu$ pair production cross section reaches to almost 1pb. On the other hand, that for $\tilde{\mu}_L$ is at most 150fb. The destructive interference between t - and s -channels reduces production of $\tilde{\mu}_L$ while the constructive interference enhances the production cross section for $\tilde{\nu}_\mu$.

In Fig. (5) we show the cross sections for $\tau^+\mu^- + \tilde{\chi}_1^-\tilde{\chi}_1^+$ by sneutrino production and $\tau^+\mu^- + \tilde{\chi}_2^0\tilde{\chi}_2^0$ by the charged slepton production at $\mu^+\mu^-$ colliders. The parameter set is the same as in Fig. (3). The cross section for $\tau^+\mu^- + \tilde{\chi}_1^-\tilde{\chi}_1^+$ by the sneutrino pair production reaches to about 75fb with full mixing, while that for $\tau^+\mu^- + \tilde{\chi}_2^0\tilde{\chi}_2^0$ by the charged slepton slepton is at most 5.6fb due to the destructive interference. As a result,

the cross sections for the signals are approximately

$$\begin{aligned}
\sigma(\tau^+\mu^- + 4\text{jets} + \cancel{E}) &\simeq 4\chi_{\tilde{\nu}} \sin^2 2\theta_{\tilde{\nu}} (1 - \chi_{\tilde{\nu}} \sin^2 2\theta_{\tilde{\nu}}) \times 30\text{fb} \\
\sigma(\tau^+\mu^- l^\pm + 2\text{jets} + \cancel{E}) &\simeq 4\chi_{\tilde{\nu}} \sin^2 2\theta_{\tilde{\nu}} (1 - \chi_{\tilde{\nu}} \sin^2 2\theta_{\tilde{\nu}}) \times 5.8\text{fb}, \\
\sigma(\tau^+\mu^- l^+ l^- + 2\text{jets} + \cancel{E}) &\simeq 4\chi_{\tilde{\nu}} \sin^2 2\theta_{\tilde{\nu}} (1 - \chi_{\tilde{\nu}} \sin^2 2\theta_{\tilde{\nu}}) \times 0.36\text{fb}.
\end{aligned} \tag{36}$$

Here, we assume the t -channel dominance in the production processes. Compared to the cross sections at LC Eq. (29), the signal cross sections at $\mu^+\mu^-$ collider is larger by one order of magnitude. A $\mu^+\mu^-$ collider is a powerful tool to study the LFV in the second generation.

4 Detecting the LFV at future e^+e^- and $\mu^+\mu^-$ colliders

4.1 Overview of signals and backgrounds

In this section, we discuss the detection of the LFV due to the $\tilde{\tau}_L - \tilde{\mu}_L$ or the $\tilde{\nu}_\tau - \tilde{\nu}_\mu$ mixing in $\tau\mu + 4\text{jets}$ and $\tau\mu l + 2\text{jet}$ modes with \cancel{E} . The branching fractions to the two modes are large, therefore they are good for the LFV study at future lepton colliders. The former signal is simple involving only two leptons in the final state, however, the mode receives the contribution from both the left-handed charged slepton and the sneutrino productions. The mixing structure of the charged sleptons is complicated involving the left-right mixing of stau's; In the previous section we saw $\tan\beta$ dependence of the signal. The latter mode receives the contribution only from $\tilde{\nu}$ production, while the signal tends to be diluted due to the third lepton l . The signal $\tau\mu l l + 4\text{jets} + \cancel{E}$ is clean, though we do not discuss it in detail here since the cross section is small.

The tau lepton pair production in the SM processes generally provides background for $\tilde{\tau}-\tilde{\mu}$ and $\tilde{\nu}_\tau-\tilde{\nu}_\mu$ mixings. For example, $Z^0W^+W^-$ production can be a background when Z decays into $\tau^+\tau^-$ and one of the two tau leptons decays into μ . The production cross section of $Z^0W^+W^-$ is about 15 fb if we require central production of gauge bosons; $|\cos\theta_V| < 0.8$ [20]. Therefore, $\sigma(l^+l^- \rightarrow Z^0(\rightarrow \tau\tau \rightarrow \mu\tau)W^+W^-) = 0.17\text{fb}$. For our sample parameter set for $\tan\beta = 3$, $\tilde{\chi}_1^-$ and $\tilde{\chi}_2^0$ do not decay into an on-shell W or Z boson, therefore we ignore this background completely, assuming jet invariant mass

cuts.⁷ Another background is $\tau^+\tau^-W^+W^-$ production where the tau lepton pair comes from initial state radiation or bremsstrahlung. The tau leptons typically have very low transverse momenta, and they can be rejected by requiring large P_T [21] to the τ candidate leptons or jets.

Rejecting backgrounds from the SUSY particle productions is also important for the LFV study. For e^+e^- colliders, the decay of sneutrino (left-handed charged slepton) pairs into $\tau^-\tilde{\chi}_1^+ (\tau^-\tilde{\chi}_2^0)$, would be important backgrounds. Decay of one of two τ 's into μ produces $\mu\tau X$ events; 17% of decaying τ 's into μ . If we cannot reject the muon, and tau leptons are identified by only the hadronic decay ($Br(\tau \rightarrow \text{hadrons}) = 65\%$), detection of the LFV at e^+e^- colliders may not be very promising. When 500 $\tau\tau X$ events are produced, $500 \times 0.64 \times 0.17 \times 2 \sim 110$ events of them will be the background $\tau\mu X$ candidates for 100 % acceptance. Then 3σ discovery of $\tilde{l}^+\tilde{l}^-$ or $\tilde{\nu}\tilde{\nu}^c \rightarrow \tau\mu X$ requires more than $\sqrt{110}/Br(\tau \rightarrow \text{hadron}) \times 3 \sim 50$ signal productions; S/N is 0.52. We need to find cuts to eliminate the background from $\tau \rightarrow \mu$ and/or to increase τ acceptance to study the LFV phenomena at e^+e^- colliders. In Section 4.2 we discuss cuts on the muon energy E_μ and the impact parameter σ_{IP} (distance between the μ track to the interaction point), and estimate the probability to misidentify μ from $\tilde{l} \rightarrow \tau$ as $\tilde{l} \rightarrow \mu$ under the cuts. The sensitivity for $\sin 2\theta_{\tilde{\nu}}$ and $\Delta m_{\tilde{\nu}}$ will be discussed in Section 4.3 for the $\tau\mu + 4\text{jets}$ mode.

For $\mu^+\mu^-$ colliders, study of the LFV would be easier because of the $\tilde{\nu}_\mu\tilde{\nu}_\mu^c$ and $\tilde{\mu}^+\tilde{\mu}^-$ productions dominate over the $\tilde{\nu}_\tau\tilde{\nu}_\tau^c$ and $\tilde{\tau}^+\tilde{\tau}^-$ productions in the limit of the small LFV. In Section 4.3, we will compare the experimental sensitivity for the LFV at $\mu^+\mu^-$ colliders to that at e^+e^- colliders. Because large statistics is expected for $\mu^+\mu^-$ colliders, we discuss the detection of the LFV in $\tau\mu l + 2\text{jets}$ mode. Some modes are masked by SUSY backgrounds such as $\mu^+\mu^- \rightarrow \tilde{\nu}\tilde{\nu}^c \rightarrow \mu^+\nu_\mu\tilde{\chi}_2^0 (\rightarrow \tau^+\tau^-)\tilde{\chi}_1^- (\rightarrow 2\text{jets})$.

4.2 Energy and impact parameter cuts

In this section we discuss cuts to eliminate $\tau\tau X$ background to $\tau\mu X$ signal. A cut on the muon energy E_μ must be very useful, and a cut on the impact parameter σ_{IP} is the other

⁷ Even if $\tilde{\chi}_1^-(\tilde{\chi}_2^0) \rightarrow W^-(Z^0)\tilde{\chi}_1^0$ is open, we can remove the background by requiring 4jet kinematics are consistent to $Z^0W^+W^-$ production. hWW production with $h \rightarrow \tau^+\tau^-$ or other Higgs boson production also must be taken into account, because the branching ratio into τ may not be negligible.

possibility if a fine vertex detector is available.

The tau lepton decays into e^- , μ^- , π^- , ρ^- , etc., and the lifetime is $c\tau_\tau = 86.93\mu m$. The decay distributions depend on the spin of the initial and the final particles. The detailed discussion on that can be found in [22] and references therein.

The decay $\tau^- \rightarrow \mu^- \nu_\tau \bar{\nu}_\mu$ involves two neutrinos, and then E_μ is significantly softer than that of the tau lepton. In Fig. (6), we show the energy distribution of μ from decaying τ when the tau lepton comes from sneutrino pair production $e^+ e^- \rightarrow \tilde{\nu} \tilde{\nu}^c$ and decay $\tilde{\nu} \rightarrow \tau^- \tilde{\chi}_1^+$ ($\tilde{\nu}^c \rightarrow \tau^+ \tilde{\chi}_1^-$). The τ energy distribution is flat between the two end points E_τ^{\min} and E_τ^{\max} ,

$$E_\tau^{\max(\min)} = E_\tau^{C.M.} (1 \pm \beta_{\tilde{\tau}}) \gamma_{\tilde{\tau}}, \quad (37)$$

where

$$E_\tau^{C.M.} = \frac{m_\nu^2 - m_{\tilde{\chi}_1^-}^2}{2m_\nu}. \quad (38)$$

Here, $\beta_\nu^2 = 1 - 4m_\nu^2/s$ and $\gamma_\nu^2 = 1/(1 - \beta_\nu^2)$, and we ignore m_τ . For our sample parameter set for $\tan\beta = 3$, $E_\tau^{\max} = 146$ GeV and $E_\tau^{\min} = 26.5$ GeV. The parent τ distribution is also shown in the plot.

The muon energy distribution has mild dependence on τ polarization P_τ , and it gets harder as P_τ is decreased. The solid line shows the distribution for $P_\tau = -1$, while the dashed line shows the distribution for $P_\tau = 1$. For the case we concern, $P_\tau \sim -1$; notice that the LFV occurs due to the mixing of left-handed sleptons in our model, and $\tilde{\chi}_1^-$ is gaugino-like in the minimal supergravity scenario, therefore the tau lepton is left-handed [23, 21].

The energy distribution for the signal μ is flat between E_μ^{\max} and E_μ^{\min} and the end points are the same to that of E_τ^{\min} and E_τ^{\max} . Therefore we can reduce the background $\tau \rightarrow \mu$ by requiring $E_\mu > E_\mu^{\min}$ without costing signal events; 52% of μ from the τ decay remains as the candidate of primary $\tilde{\nu} \rightarrow \mu$ decay if we require $E_\mu > E_\mu^{\min}$. Though increasing E_μ^{cut} reduces signal, S/N would be improved considerably. For $E_\mu^{\text{cut}} = 50(70)$ GeV, 25%(1%) of $\tau \rightarrow \mu$ remains and the S/N ratio is improved by a factor of 3(90) to that without the cut.

We now consider a cut on σ_{IP} . The measurement of the distance σ_{IP} using a vertex detector might be useful to reduce background. The μ from the signal $e^+ e^- \rightarrow \tilde{l}^- \tilde{l}^+$ or $\tilde{\nu} \tilde{\nu}^c$

$\rightarrow \tau \mu \tilde{\chi} \tilde{\chi}$ must have a track which points back toward the interaction point. By requiring signal event to have $\sigma_{IP} < \sigma_{IP}^{\text{cut}}$ one can eliminate some backgrounds.

When a relativistic τ lepton is produced at an interaction point, it flies for length l and then decays. The decay distribution may be obtained by boosting the decay distribution at the τ rest frame. Let us denote the muon momentum at the τ rest frame as $(E^0, p_{T1}^0, p_{T2}^0, p_{/\!/}^0)$, where $p_{/\!/}^0$ is the component parallel to the boosted direction. When $p_{/\!/}^0$ is large and positive, the daughter μ energy is large in the laboratory frame, namely, by ignoring m_μ ,

$$E_\mu = (\beta_\tau p_{/\!/}^0 + E^0) \gamma_\tau. \quad (39)$$

The angle between μ and τ momenta in the laboratory frame is

$$\tan \theta = \frac{|p_T^0|}{(p_{/\!/}^0 + \beta_\tau E^0) \gamma_\tau}. \quad (40)$$

Apparently, when the τ energy is large, θ is small. However the average τ flight length increases proportional to γ_τ , typically $l \sim \gamma_\tau \beta_\tau c \tau_\tau$. Therefore the measurable quantity σ_{IP} is

$$\begin{aligned} \langle \sigma_{IP} \rangle &= \langle l \sin \theta \rangle \\ &\sim c \tau_\tau \frac{\beta_\tau |p_T^0|}{(p_{/\!/}^0 + \beta_\tau E^0)}. \end{aligned} \quad (41)$$

Notice that γ_τ dependence is now disappeared. In the $\beta_\tau \sim 1$ limit, σ_{IP} distribution depends only on the μ decay distribution in the rest frame. Unless $\beta_\tau \ll 1$, σ_{IP} tends to be smaller than $c \tau_\tau$, because $E^0 > |p_T^0|$. The E_μ and σ_{IP} distributions may be obtained by numerically convoluting the distributions for τ decaying into μ with the parent τ energy distribution. The detailed formula is given in the Appendix E

Fine vertex resolution might be achieved at future e^+e^- LC experiments. For the JLC1 detector, a CCD vertex detector is proposed, and the impact parameter resolution $\delta\sigma$ is estimated as $\delta\sigma = 11.4 \oplus 28.8/p\beta/\sin^{3/2}\theta(\mu m)$ [24]. The recent NLC detector study shows $\delta\sigma = 2.4 \oplus 13.7/p\beta/\sin^{3/2}\theta(\mu m)$ is possible [25]. For $\mu^+\mu^-$ colliders, the proper configuration of the detector is still under preliminary consideration. Large backgrounds of electrons, photons, pions, and muon's are expected near the interaction region. Because the large signal cross section is expected for muon colliders, we can expect good experimental sensitivity to the LFV without an IP cut.

It is important to have $\delta\sigma_{IP} \ll c\tau_\tau$, as σ_{IP} is very likely less than $c\tau_\tau$. Notice that the error on the σ_{IP} is estimated about $2.5\mu m$ at $E_\mu \sim E_\mu^{\min}$ in the NLC detector. If the interaction point is well-known, $\sigma_{IP}^{\text{cut}} \sim 10\mu m$ sounds reasonable choice. One question is if the interaction point is determined accurately enough. The particles contained in the jets are generally softer than the parton energy, therefore the σ_{IP} resolution of each track in the jets is less accurate. The resolution of interaction point will be determined by combining the each track measurement. The estimation of the resolution requires detailed detector studies, which are out of scope of this paper. Even if the interaction point cannot be measured precisely, the beam position must be very accurately known for LC's. One might try to measure the distance between the μ track and the beam axis, although it generally gives poor results than the one given here.

In Fig. (7), we show the energy distribution of μ from $\tilde{\nu} \rightarrow \tau \rightarrow \mu$ decay requiring $\sigma_{IP} < \sigma_{IP}^{\text{cut}} = 10, 30, 50, 90\mu m$. The background decreases as one require a tighter σ_{IP} cut. Notice that the background is not reduced too much when E_μ is close to E_μ^{\max} . In such a case as $|p_T^0| \ll |p_{\parallel}^0|$, the typical σ_{IP} is smaller as can be seen from Eq. (41). In Fig. (8) we show E_μ distribution for $\sigma_{IP} < \sigma_{IP}^{\text{cut}}$ as a ratio to E_μ distribution without the σ_{IP} cut. We see the moderate reduction of the background in the wide range of E_μ , which helps to improve the S/N ratio without reducing signal events. If we require σ_{IP} is less than $10\mu m$, the background is reduced by a factor of 6 at $E_\mu \sim E_\mu^{\min}$.

The σ_{IP}^{cut} cut is attractive in the sense to increase S/N without costing signal events. In Fig. (9) we plot p_μ , the probability that $\tilde{\nu}$ production and its decay into τ is mis-identified as $\tilde{\nu} \rightarrow \mu\tilde{\chi}$. We assume that μ from direct $\tilde{f} \rightarrow \mu\tilde{\chi}$ decay is selected when following conditions are satisfied;

- $E_\mu^{\min} < E_\mu < E_\mu^{\max}$,
- $\sigma_{IP} < \sigma_{IP}^{\text{cut}}$.

Isolated hard low multiplicity jets will be identified as τ . We assume all the hadronic decay of τ are identified as τ candidates. In addition, the leptons with $\sigma_{IP} > \sigma_{IP}^{\text{cut}}$ may be regarded as τ candidates, too. We define the τ identification probability p_τ as

$$p_\tau = 0.64 + 0.35 \times p, \quad (42)$$

where p is the probability that lepton from decaying τ has $\sigma_{IP} > \sigma_{IP}^{\text{cut}}$ and $E_l > 5 \text{ GeV}$.⁸ We show p_τ in Table (6) with p_μ .

Isolation cuts for the leptons and other cuts must be applied to select signal events. They may be taken care as an overall acceptance common to $\tau\tau$, $\mu\mu$ and $\tau\mu$ events. We discuss them in the next subsection.

4.3 $\tau\mu + 4\text{jets}$ mode

We first discuss $\tau\mu + 4\text{jets}$ mode with \cancel{E} . The mode has large branching ratio, and the interpretation of signal is simple. In the limit of zero flavor mixing, $\mu\mu + 4\text{jets}$ event will be produced around 120fb for muon colliders, and 2.5fb for e^+e^- colliders. The signal $\tau\mu + 4\text{jets}$ candidates will be selected by the E_μ^{cut} and the IP cuts discussed in the previous subsection, and we assume backgrounds dominantly come from $\tau^+\tau^- + 4\text{jets} + \cancel{E}$ production. The background can be subtracted by simultaneously measuring the cross section.

The significance of the signal \mathcal{S} is a function of accepted numbers of $\tau\mu + 4\text{jets} + \cancel{E}$ and $\tau\tau + 4\text{jets} + \cancel{E}$ events $O_{\tau\mu}$ and $O_{\tau\tau}$. When statistics of the signal and the background is large, we can assume Gaussian distribution and

$$\mathcal{S} = O_{\text{sig}}/\delta O_{\text{sig}}, \quad (43)$$

where

$$(\delta O_{\text{sig}})^2 = O_{\tau\mu} + 4(p_\mu/p_\tau)^2 O_{\tau\tau}. \quad (44)$$

Here p_μ and p_τ are the μ misidentification rate and the τ identification rate discussed before, and $O_{\text{sig}} = O_{\tau\mu} - O_{\text{bg}}$, where O_{bg} is estimated as $O_{\text{bg}} = (p_\mu/p_\tau)O_{\tau\tau}$. The $O_{\tau\tau}$ and O_{sig} are related to the signal cross section by

$$\begin{aligned} O_{\tau\tau} &= A_{\tau\tau} p_\tau p_\tau N_{\tau\tau}, \\ O_{\text{sig}} &= A_{\tau\mu} p_\tau (N_{\tau\mu} + N_{\mu\tau}), \end{aligned} \quad (45)$$

⁸We need to veto soft jets or leptons to reject soft particles from jets. The hadronic τ decay product carries a substantial fraction of τ energy when the mass of the decay products is of the order of m_τ , therefore effect of the energy cut is small.

and

$$N_{l_i l_j}^{e(\mu)} = \mathcal{L} \times \sigma(e^+ e^- (\mu^+ \mu^-) \rightarrow \tilde{l}^- \tilde{l}^+ \text{ or } \tilde{\nu} \tilde{\nu}^c \rightarrow l_i^+ l_j^- + 4\text{jets} + \cancel{E}), \quad (46)$$

where \mathcal{L} is the integrated luminosity and A_{ij} is the acceptance of $\tau\tau(\tau\mu) + 4\text{jets}$ modes.

Notice that we add signals from the sneutrino and the charged slepton productions. This is because $m_{\tilde{\nu}} \sim m_{\tilde{l}_L}$ and $m_{\tilde{\chi}_2^0} \sim m_{\tilde{\chi}_1^-}$, therefore $\tau\mu + 4\text{jets}$ events from the charged slepton and sneutrino productions have similar kinematical signature. The muon misidentification rate p_μ depends on primary μ criteria which is specified by the E_μ^{cut} and σ_{IP}^{cut} . The energy distribution of μ from $\tilde{\nu}/\tilde{l} \rightarrow \tau \rightarrow \mu$ depends on the charged slepton and the sneutrino masses, and the chargino and neutralino masses, therefore p_μ is a function of those masses. However, in our model, the energy distributions of μ from different decay chains are similar, so we choose common p_μ for charged slepton and sneutrino backgrounds to estimate the experimental sensitivity. For LC's we take $p_\mu = 0.02$ and $p_\tau = 0.88$ for $\sigma_{IP}^{\text{cut}} = 10\mu\text{m}$. For muon colliders, we use the value without the IP cut, $p_\mu = 0.09$ and $p_\tau = 0.64$.

The slepton mass uncertainty is removed by studying the end point energy of electron or muon from $\tilde{\nu}_{e(\mu)}$ decay. The production cross section of $\tilde{\nu}_{e(\mu)}$ is large at $e^+ e^- (\mu^+ \mu^-)$ colliders, and one can determine the masses of sneutrino and chargino very precisely by the method [15, 26]. The mass resolution of 2% for the $\tilde{\nu}$ is straightforward if the cross section is of the order of 1 pb. The \tilde{e}_L and $\tilde{\mu}_L$ productions should also give us the information on the left-handed charged slepton masses.

No Monte Carlo (MC) study involving $\tilde{\tau}_L$ and $\tilde{\nu}_\tau$ has been done. Therefore we seek for a reasonable assumption for A_{ij} . Those acceptances are again in principle different between the signals from $\tilde{\nu}$ and \tilde{l} productions, however, we assumed that they are universal because of the kinematical similarity of the mode. The MC study of the process $\tilde{\tau}_R^+ \tilde{\tau}_R^- \rightarrow \tau^+ \tau^- \tilde{\chi}_1^0 \tilde{\chi}_1^0$ has been done in Ref. [21] without assuming a vertex detector. In the paper, the tau jets are identified by suitable multiplicity cuts, jet invariant mass cuts, and no substantial reduction of the signal events coming from the τ identification was found. However, the isolation cut from other jet activities for τ and μ candidates has to be required for our case, and it might reduce accepted events. On the other hand, the SM backgrounds for the signal of the left handed slepton production are substantially smaller

than that for the $\tilde{\tau}_R^+ \tilde{\tau}_R^-$ production case because of the multiple jets in the final state, and we do not need strong kinematical cuts applied in Ref. [21]. Indeed, for the $\tilde{\nu}$ study in Ref. [15], the acceptance is found around 50%, higher than those typical for $\tilde{\chi}_1^-$ or \tilde{l}_R studies, 30%. We therefore assume 30% as the overall acceptance A to the signal.

Now we are ready to estimate experimental sensitivity for the LFV process based on Eq. (43). In Fig. (10) we plotted the contours of constant significance corresponding to 3σ discovery in $\sin 2\theta_{\tilde{\nu}}$ and $\Delta m_{\tilde{\nu}}$ plain. We take the sample parameter set for $\tan \beta = 3$ in Table (1), and parameterize the sneutrino mass matrix by $\sin 2\theta_{\tilde{\nu}}$ and the mass splitting between two non-electron sneutrinos $\Delta m_{\tilde{\nu}}$. We assume the integrated luminosity $\mathcal{L} = 50\text{fb}^{-1}$, proposed one year luminosity of LC's. For the e^+e^- colliders, the experimental sensitivity is limited by the small statistics of the signal. The parameter region with $\sin 2\theta_{\tilde{\nu}} > 0.5$ and $\Delta m_{\tilde{\nu}} > 0.4$ GeV may be explored. However, the background is strongly suppressed by the factor of $p_\mu = 0.02$ (corresponds to $\sigma_{IP}^{\text{cut}} = 10\mu\text{m}$.) Provided accidental backgrounds (such as τ lepton off from a charm jet) can be controlled, the sensitivity may be extended up to the region where $S/N \sim 1$. (That corresponds to the region $\sin 2\theta_{\tilde{\nu}} > 0.2$ and $\Delta m_{\tilde{\nu}} > 0.1$ GeV in our sample parameter).

For the case of $\mu^+\mu^-$ collisions, the signal rate is a factor 10 larger than e^+e^- collisions as shown in Fig. (10). Notice that S/N in the small mixing region is enhanced due to the enhanced $\mu^+\mu^- + 4\text{jets} + \cancel{E}$ rate over the background $\tau^+\tau^- + 4\text{jets} + \cancel{E}$ rate. The region where $\sin(2\theta_{\tilde{\nu}}) > 0.1$ GeV or $\Delta m_{\tilde{\nu}} > 0.1$ can be explored for the integrated luminosity $\mathcal{L} = 50\text{fb}^{-1}$.

4.4 $\tau\mu l + 2\text{jets}$ modes

The signal $\tau\mu + 4\text{jets} + \cancel{E}$, which we considered in the previous section, involves many jets in the final state. Since large fraction of the τ leptons is detected by the hadronic decays, and the background from $c \rightarrow \tau$ off the jet axis could be large. This means that we might need very tight isolation cuts, resulting poor acceptance. Therefore it is useful to search for the LFV in $\tau\mu l + 2\text{jets}$ modes. Notice that the process is induced by only $\tilde{\nu}$ production involved as shown in Eq. (3). The detection of the LFV in these modes might provide clean information on the sneutrino mass matrix.

The search of $\tau\mu l + 2\text{jets}$ modes at muon colliders would be promising, because the

production cross section for $\tilde{\nu}_\mu \tilde{\nu}_\mu^c$ is enhanced. The total cross section for $(\mu^+ \mu^- l + 2jets)$ is 140 fb for our sample parameter set for $\tan\beta = 3$ when the mixing is small. The cross section for $\tau^\pm \mu^\mp l + 2jets$ will be suppressed by a factor of $\sin^2 2\theta_{\tilde{\nu}}$ to the large cross section for $\mu^+ \mu^- l + 2jets$ when the sneutrino mass difference is large enough.

There are several sources of SUSY backgrounds to the signals. The sneutrino and the charged slepton decays into neutrino cause $3l$ signal. The dominant one is

$$\begin{aligned} \tilde{\nu} \tilde{\nu}^c &\rightarrow \mu^- \bar{\nu} + \tilde{\chi}_1^+ \tilde{\chi}_2^0 \\ &\quad \left\{ \begin{array}{l} \tilde{\chi}_1^+ \rightarrow 2jets + \tilde{\chi}_1^0 \\ \tilde{\chi}_2^0 \rightarrow \tau^+ \tau^- + \tilde{\chi}_1^0 \end{array} \right. \quad (6.6\text{fb}), \end{aligned} \quad (47)$$

$$\begin{aligned} \tilde{l}^- \tilde{l}^+ &\rightarrow \mu^- \bar{\nu} + \tilde{\chi}_2^0 \tilde{\chi}_1^+ \\ &\quad \left\{ \begin{array}{l} \tilde{\chi}_2^0 \rightarrow \tau^+ \tau^- + \tilde{\chi}_1^0 \\ \tilde{\chi}_1^+ \rightarrow 2jets + \tilde{\chi}_1^0 \end{array} \right. \quad (2.8\text{fb}). \end{aligned} \quad (48)$$

Those are the backgrounds from the charged slepton or the sneutrino decay into μ , which have large cross sections in the limit of the small LFV. (The production cross sections in zero LFV limit are listed at the end of Eqs. (47,48).)

Notice that the energy distribution of μ from the primary slepton decay in Eqs. (47,48) is similar to that of the signal, therefore it is not possible to reduce the background by the E_μ cuts. The situation is different to the previous $\tau \mu + 4jets$ study. For the previous case the background can be reduced because of the soft energy spectrum of μ from the τ decay.

Because of the background, the $\tau^\pm \mu^\mp \tau^\mp$ modes and $\tau^\pm \mu^\mp \mu^\mp (\text{e}^\mp)$ are not promising.⁹ In the limit of the small LFV, S/N for $\tau^\pm \mu^\mp \tau^\mp$ would not go too much above $1/2(\sin 2\theta_{\tilde{\nu}})^2 \times \sigma(\mu^+ \mu^- \tilde{\chi}_1^+ (\rightarrow \tau^+) \tilde{\chi}_1^-)|_{\text{no-mixing}} / \sigma(\nu \mu^- \tilde{\chi}_2^0 (\rightarrow \tau^+ \tau^-) \tilde{\chi}_1^+)|_{\text{no-mixing}} \sim 1.2(\sin 2\theta_{\tilde{\nu}})^2$. For $\tau^\pm \mu^\mp \mu^\mp$ and $\tau^\pm \mu^\mp \text{e}^\mp$ modes, the background will be suppressed by τ branching ratio into μ or e , however, those modes are not attractive compared to the modes we discuss below.

The modes $\tau^\pm \mu^\mp l^\pm + 2jets$ ($l \equiv \tau, \mu, \text{e}$) do not suffer large background contribution from $\mu^\mp \nu(\bar{\nu}) \tilde{\chi}_1^0 \tilde{\chi}_1^\pm$ production. Therefore we discuss the modes rather carefully.

- $\tau^+ \tau^+ \mu^- + 2jets$ mode

⁹s The background τ energy distribution from $\tilde{\chi}_1^0$ decay may be softer than signal. However, the cut to E_τ would not be too efficient because the energy distribution is smeared by τ decay.

For $\tau^+\tau^+\mu^-$ mode, the signal comes from sneutrino pair decay into $\tau^+\tilde{\chi}_1^-\mu^-\tilde{\chi}_1^+$ followed by decay of $\tilde{\chi}_1^+$ into $\tau^+\nu\tilde{\chi}_1^0$ and that of $\tilde{\chi}_1^-$ into $2jets\tilde{\chi}_1^0$. Those three leptons in the final state must be identified correctly. Backgrounds are expected from

$$(A) \quad \mu^+\mu^- \rightarrow \tilde{l}^+\tilde{l}^- \text{ or } \tilde{\nu}\tilde{\nu}^c \rightarrow \tau^+\nu + \tilde{\chi}_2^0\tilde{\chi}_1^- \quad \left\{ \begin{array}{l} \tilde{\chi}_2^0 \rightarrow \tau^+\tau^-(\rightarrow \mu^-) + \tilde{\chi}_1^0 \\ \tilde{\chi}_1^- \rightarrow 2jets + \tilde{\chi}_1^0 \end{array} \right. \quad (49)$$

and

$$(B) \quad \mu^+\mu^- \rightarrow \tilde{\nu}\tilde{\nu}^c \rightarrow \tau^+\tau^-(\rightarrow \mu^-) + \tilde{\chi}_1^+\tilde{\chi}_1^- \quad \left\{ \begin{array}{l} \tilde{\chi}_1^+ \rightarrow \tau^+\nu_\tau + \tilde{\chi}_1^0 \\ \tilde{\chi}_1^- \rightarrow 2jets + \tilde{\chi}_1^0 \end{array} \right. \quad (50)$$

with misidentification of $\tau^- \rightarrow \mu^-$ as primary μ^- . The background cross sections are small in the limit of zero slepton mixing since they are induced by the $\tilde{\tau}_L$ or $\tilde{\nu}_\tau$ production. If the mixing is non-zero, the t -channel chargino or neutralino exchange contribution to them is suppressed by a factor proportional to $\sin^2 \theta_{\tilde{\nu}}$ for (A), and $\sin^4 \theta_{\tilde{\nu}}$ for (B). For background (A), τ from $\tilde{\chi}_2^0$ decay must have soft energy spectrum, therefore μ from the τ decay, too. We assume the background (A) will be negligible if a moderate E_μ cut is applied. The rejection of background (B) is analogous to the $\tau\mu + 4jets$ mode.

- $\tau^+e^+\mu^- + 2jets$ mode

The background from

$$\mu^+\mu^- \rightarrow \tilde{l}^+\tilde{l}^- \text{ or } \tilde{\nu}\tilde{\nu}^c \rightarrow \tau^+\nu + \tilde{\chi}_2^0\tilde{\chi}_1^+ \quad \left\{ \begin{array}{l} \tilde{\chi}_2^0 \rightarrow \tau^+(\rightarrow e^+)\tau^-(\rightarrow \mu^-) + \tilde{\chi}_1^0 \\ \tilde{\chi}_1^+ \rightarrow 2jets + \tilde{\chi}_1^0 \end{array} \right. \quad (51)$$

is doubly suppressed by τ branching ratio into lepton, and the muon is very soft. The misidentification of primary $\tau^+\tau^-$ as primary $\tau\mu$

$$\mu^+\mu^- \rightarrow \tilde{\nu}\tilde{\nu}^c \rightarrow \tau^+\tau^-(\rightarrow \mu^-) + \tilde{\chi}_1^+\tilde{\chi}_1^- \quad \left\{ \begin{array}{l} \tilde{\chi}_1^+ \rightarrow e^+\nu_e + \tilde{\chi}_1^0 \\ \tilde{\chi}_1^- \rightarrow 2jets + \tilde{\chi}_1^0 \end{array} \right. \quad (52)$$

would be the dominant background.

In the limit of the small LFV, the signal dominates over the background for the above two process. The statistics of the signal will be estimated by

$$S = \mathcal{L} \times 2A(p_\tau^2 + p_\tau)\sigma \left(\tau^+ \mu^- \tilde{\chi}_1^+ (\rightarrow l^+) \tilde{\chi}_2^0 (\rightarrow 2\text{jets}) \right), \quad (53)$$

since the background is negligible. In Section 4.2 we take $p_\tau = 0.64$ if we use only the energy cut. Assuming t -channel dominance for the production cross section, 3σ discovery of signal corresponds to $\sin 2\theta_{\tilde{\nu}} = 0.15$ for $\mathcal{L} = 50 \text{ fb}^{-1}$ and $A = 0.3$.

It is not clear if $\tau^+ \mu^- \mu^+$ mode is usable. The background from sneutrino flavor conserving decay

$$\begin{aligned} \mu^+ \mu^- \rightarrow \tilde{\nu} \tilde{\nu}^c \rightarrow \mu^+ \mu^- \tilde{\chi}_1^\pm \tilde{\chi}_1^\mp \\ \left\{ \begin{array}{l} \tilde{\chi}_1^\pm \rightarrow \tau^\pm \nu (\bar{\nu}) + \tilde{\chi}_1^0 \\ \tilde{\chi}_1^\mp \rightarrow 2\text{jets} + \tilde{\chi}_1^0 \end{array} \right. \quad (23\text{fb}) \end{aligned} \quad (54)$$

is large, and would be an important background for this case. Both of the μ 's in the background process have energy between E_μ^{\min} and E_μ^{\max} . Therefore the cut $E_\mu^{\text{soft}} < E_\mu^{\min} < E_\mu^{\text{hard}}$, will remove the background Eq. (54) completely. The cut will remove some signal events, and the signal acceptance depends on the decay distribution of $\tilde{\chi}_1^\pm$. The background from $\tau^+ \nu \tilde{\chi}_2^0 (\rightarrow \mu^+ \mu^-) \tilde{\chi}_1^+ (\rightarrow 2\text{jets})$ may also be significant because muons come directly from the $\tilde{\chi}_2^0$ decay, unlike the two modes discussed previously, while the cross section is suppressed only by a factor of $\sin^2 2\theta_{\tilde{\nu}}$. To remove the background, we may have to increase the energy cut for the harder muon. The MC simulation is needed to obtain S/N ratio with the optimized cuts for this mode.

5 Conclusion and Discussion

In this paper we discuss the detection of the LFV expected in the MSSMR at future lepton colliders. We assume ν_τ - ν_μ mixing inspired by the Super-Kamiokande atmospheric results. In the model, the LFV is induced in the left-handed slepton mass matrix radiatively. As a result, the charged sleptons and the sneutrinos in the second and third generations mix, and the LFV may be observed by measuring the slepton production and their decay; $\mu^+ \mu^- (\text{e}^+ \text{e}^-) \rightarrow \tilde{\nu} \tilde{\nu}^c \rightarrow \tau \mu \tilde{\chi}_1^+ \tilde{\chi}_1^-$ and $\mu^+ \mu^- (\text{e}^+ \text{e}^-) \rightarrow \tilde{l}^+ \tilde{l}^- \rightarrow \tau \mu \tilde{\chi}_2^0 \tilde{\chi}_2^0$ where $\tilde{\chi}_1^\pm$ and $\tilde{\chi}_2^0$ decay into leptons or jets with the LSP further.

For e^+e^- colliders, the signal cross section is small because only s -channel exchange of gauge boson is involved. The $\tilde{\nu}_\tau \tilde{\nu}_\tau^c (\tilde{\tau}^+ \tilde{\tau}^-)$ production and the decay into $\tau\tau + \tilde{\chi}_1^+ \tilde{\chi}_1^- (\tilde{\chi}_2^0 \tilde{\chi}_2^0)$ would be significant background if we do not veto μ from the τ decay. In this paper, we point out that the background events would be reduced drastically by requiring $E_\mu^{\text{cut}} \geq E_\mu^{\text{min}}$, where E_μ^{min} is the minimum muon energy for the signal events. Furthermore σ_{IP} , the distance of the muon track from the interaction point, can be measured precisely for future LC detectors. Requiring $\sigma_{IP} \ll c\tau_\tau$ to $\tau\mu X$ events we can improve the S/N ratio further. For one year of luminosity $\mathcal{L} = 50\text{fb}^{-1}$, $\sin 2\theta_{\tilde{\nu}} \gtrsim 0.5$ and $\Delta m_{\tilde{\nu}} \gtrsim 0.4\text{GeV}$ may be explored in the mode $\tau\mu + 4\text{jets}$. The experimental reach is limited by statistics only.

At $\mu^+\mu^-$ colliders, the signal cross sections are enhanced by the t -channel exchange of charginos or neutralinos. In the limit of the small LFV, the production cross sections for the third generation sfermions involve only s -channel diagrams, therefore the background is relatively suppressed. $\sin 2\theta_{\tilde{\nu}} \gtrsim 0.1$ and $\Delta m_{\tilde{\nu}} \gtrsim 0.1\text{GeV}$ may be explored in the mode $\tau\mu + 4\text{jets}$ without the σ_{IP} cut.

The $\tau\mu + 4\text{jets}$ mode receives contribution both from the $\tilde{\nu}$ and \tilde{l} productions. The \tilde{l} mass matrix is rather complicated, depending on the $\tilde{\tau}_L$ - $\tilde{\tau}_R$ mixing. On the other hand, the $\tau\mu l + 2\text{jets}$ modes receive the contribution only from the sneutrino production, therefore theoretically clean. We discussed the study of the modes at $\mu^+\mu^-$ colliders. Unfortunately, the half of the decay modes are masked by SUSY backgrounds.

Because the decay of the third generation sleptons involves τ leptons and jets, special attention must be paid to the τ isolation cuts. No serious MC simulation involving $\tilde{\tau}_L$ and $\tilde{\nu}_\tau$ has been done so far. In this paper, we simply assumed overall acceptance of 30%. The isolation cuts may alter the acceptance by a factor, but we expect the problem is less severe for $\tau\mu l + 2\text{jets}$ modes.

We did not discuss all discovery modes in this paper. For example the processes $\tilde{l}\tilde{l} \rightarrow \tau\mu\tilde{\chi}_2^0 (\rightarrow ll)\tilde{\chi}_2^0 (\rightarrow 2\text{jets})$ must be a clean mode sensitive to the LFV in the \tilde{l} mass matrix. The branching ratio of the modes depends on $\tan\beta$ sensitively through $Br(\tilde{\chi}_2^0 \rightarrow 2l)$. We also did not discuss the case where \tilde{l} decays dominantly into $l\tilde{\chi}_1^0$ since the region where $m_{\tilde{l}_L}, m_{\tilde{\nu}} < m_{\tilde{\chi}_1^-}, m_{\tilde{\chi}_2^0}$ is expected to be very narrow in the minimal supergravity scenario. In the case, the signal is $\tau\mu + \cancel{E}$. The mode suffers background from W pair production unless high beam polarization is available in LC's. In $\mu^+\mu^-$ colliders the signal may be

accessible due to the high statistics. We did not discuss τ -e mixing, which is not favored by current experimental data for neutrinos.

Atmospheric neutrino study implies that the Yukawa sector of lepton could be completely different from that of quark. Namely large mixing is expected between the second and third generations for lepton, while it is very small for quark mass matrix. If this implies existence of the large LFV Yukawa interaction between the third and second generations, it leads to the LFV signal in the slepton production in the seesaw mechanism. We emphasize that a $\mu^+\mu^-$ collider stands as a powerful tool to explore it in future.

Acknowledgment

The authors would like to thank Dr. Y. Okada, Dr. K. Fujii, and Dr. A. Miyamoto. This work is supported in part by Grants in aid for Science and Culture of Japan (No.10740133, No.10140211, and No.10140216).

A Lagrangian of the MSSM with Flavor Violations

In this Appendix, we present the Lagrangian of the MSSM. The superpotential in the MSSM is given by

$$W = f_l^{ij} H_1 E_i^c L_j + f_d^{ij} H_1 D_i^c Q_j + f_u^{ij} H_2 U_i^c Q_j + \mu H_1 H_2 \quad (55)$$

where L_i represents the chiral multiplet of an $SU(2)_L$ doublet lepton, E_i^c an $SU(2)_L$ singlet charged lepton, H_1 and H_2 two Higgs doublets with opposite hypercharge. Similarly Q , U^c and D^c represent chiral multiplets of quarks of an $SU(2)_L$ doublet and two singlets with different $U(1)_Y$ charges. The subscripts i and j are for generation. In this article we ignore the CKM mixing for quark sector, which is irrelevant for our discussion.

The soft SUSY breaking terms are given as

$$\begin{aligned} -\mathcal{L}_{soft} = & (m_{\tilde{Q}}^2)_i^j \tilde{q}_L^{\dagger i} \tilde{q}_{Lj} + (m_{\tilde{u}}^2)_j^i \tilde{u}_{Ri}^* \tilde{u}_R^j + (m_{\tilde{d}}^2)_j^i \tilde{d}_{Ri}^* \tilde{d}_R^j \\ & + (m_{\tilde{L}}^2)_i^j \tilde{l}_L^{\dagger i} \tilde{l}_{Lj} + (m_{\tilde{e}}^2)_j^i \tilde{e}_{Ri}^* \tilde{e}_R^j + \tilde{m}_{h1}^2 h_1^\dagger h_1 + \tilde{m}_{h2}^2 h_2^\dagger h_2 \\ & + (B\mu h_1 h_2 + h.c.) \\ & + (A_d^{ij} h_1 \tilde{d}_{Ri}^* \tilde{q}_{Lj} + A_u^{ij} h_2 \tilde{u}_{Ri}^* \tilde{q}_{Lj} + A_l^{ij} h_1 \tilde{e}_{Ri}^* \tilde{l}_{Lj} + h.c.) \\ & + \frac{1}{2} M_1 \tilde{B} \tilde{B} + \frac{1}{2} M_2 \tilde{W} \tilde{W} + \frac{1}{2} M_3 \tilde{G} \tilde{G} + h.c.). \end{aligned} \quad (56)$$

Here, the first two lines are soft terms for sleptons, squarks, and the Higgs bosons, and the third and fourth lines are those for a supersymmetric mass and Yukawa interactions, while the last line gives gaugino mass terms.

B Interaction of SUSY particles

In this Appendix, we give our notations and conventions for masses and vertices relevant for our calculation. First, we discuss quarks and leptons. We denote by l_i , u_i , and d_i the fermion mass eigenstates with m_{f_i} ($f = l, u, d$). As for the neutrinos, their masses are small and negligible. In our convention, ν_i is the $SU(2)_L$ isodoublet partner to e_{Li} .

Next, we consider sfermions. Let \tilde{f}_{Li} and \tilde{f}_{Ri} be the superpartners of f_{Li} and f_{Ri} , respectively. Here, f stands for l , u , or d . The sfermion mass matrix can be written in

the following form,

$$\left(\tilde{f}_L^\dagger, \tilde{f}_R^\dagger \right) \begin{pmatrix} m_L^2 & m_{LR}^{2\top} \\ m_{LR}^2 & m_R^2 \end{pmatrix} \begin{pmatrix} \tilde{f}_L \\ \tilde{f}_R \end{pmatrix}, \quad (57)$$

where m_L^2 and m_R^2 are (3×3) hermitian matrices and m_{LR}^2 is a 3×3 matrix. These elements are given from Eqs. (55,56) as following,

$$m_L^2 = m_{\tilde{f}_L}^2 + m_f^2 + m_Z^2 c_{2\beta} (T_{3L}^f - Q_{em}^f s_W^2), \quad (58)$$

$$m_R^2 = m_{\tilde{f}_R}^2 + m_f^2 + m_Z^2 c_{2\beta} Q_{em}^f s_W^2, \quad (59)$$

$$m_{LR}^2 = \begin{cases} -A_f v s_\beta / \sqrt{2} - m_f \mu / t_\beta & (f = u), \\ A_f v c_\beta / \sqrt{2} - m_f \mu t_\beta & (f = d, l), \end{cases} \quad (60)$$

where T_{3L}^f and Q_{em}^f are the weak isospin and the electric charge, respectively. Here, $m_{\tilde{f}_Q}^2 = m_Q^2$ for squarks, $m_{\tilde{f}_L}^2 = m_L^2$ for sleptons, and $m_{\tilde{f}_R}^2$ are each right-handed sfermion soft-breaking mass. The vacuum expectation values for the Higgs doublets are given as $\langle h_1 \rangle = (v \cos \beta, 0)^T$ and $\langle h_2 \rangle = (0, v \sin \beta)^T$.¹⁰ We assume the above mass matrix to be real. This is, in general, not diagonal, and includes mixing between different generations. For charged sleptons and squarks, we diagonalize the mass matrix $M_{\tilde{f}}^2$ by a (6×6) real orthogonal matrix U^f as

$$U^f M_{\tilde{f}}^2 U^{f\top} = (\text{diagonal}), \quad (61)$$

and we denote its eigenvalues by $m_{\tilde{f}_X}^2$ ($X = 1, \dots, 6$). The mass eigenstates are then written as

$$\tilde{f}_X = U_{X,i}^f \tilde{f}_{Li} + U_{X,i+3}^f \tilde{f}_{Ri}, \quad (X = 1, \dots, 6). \quad (62)$$

Conversely, we have

$$\tilde{f}_{Li} = U_{iX}^{f\top} \tilde{f}_X = U_{X,i}^f \tilde{f}_X, \quad (63)$$

$$\tilde{f}_{Ri} = U_{i+3,X}^{f\top} \tilde{f}_X = U_{X,i+3}^f \tilde{f}_X. \quad (64)$$

An attention should be paid to the neutrinos since the MSSM has no right-handed sneutrino. Let $\tilde{\nu}_{Li}$ be the superpartner of the neutrino ν_i . The mass eigenstate $\tilde{\nu}_X$ ($X = 1, 2, 3$) is related to $\tilde{\nu}_{Li}$ as

$$\tilde{\nu}_{Li} = U_{Xi}^\nu \tilde{\nu}_X. \quad (65)$$

¹⁰ For simplicity, we denote $\sin \beta$ and $\cos \beta$ as s_β and c_β in equations. Similarly, s_W and c_W are for the Weinberg angle, $\sin \theta_W$ and $\cos \theta_W$.

We now turn to charginos. The chargino mass matrix is given by

$$-\mathcal{L}_m = \left(\overline{\tilde{W}_R^-} \ \overline{\tilde{H}_{2R}^-} \right) \begin{pmatrix} M_2 & \sqrt{2}m_W c_\beta \\ \sqrt{2}m_W s_\beta & \mu \end{pmatrix} \begin{pmatrix} \tilde{W}_L^- \\ \tilde{H}_{1L}^- \end{pmatrix} + h.c.. \quad (66)$$

This matrix M_C is diagonalized by (2×2) real orthogonal matrices O_L and O_R as

$$O_R M_C O_L^\top = (\text{diagonal}). \quad (67)$$

Define

$$\begin{pmatrix} \tilde{\chi}_{1L}^- \\ \tilde{\chi}_{2L}^- \end{pmatrix} = O_L \begin{pmatrix} \tilde{W}_L^- \\ \tilde{H}_{1L}^- \end{pmatrix}, \quad \begin{pmatrix} \tilde{\chi}_{1R}^- \\ \tilde{\chi}_{2R}^- \end{pmatrix} = O_R \begin{pmatrix} \tilde{W}_R^- \\ \tilde{H}_{2R}^- \end{pmatrix}. \quad (68)$$

Then

$$\tilde{\chi}_A^- = \tilde{\chi}_{AL}^- + \tilde{\chi}_{AR}^-, \quad (A = 1, 2), \quad (69)$$

forms a Dirac fermion with the mass $M_{\tilde{\chi}_A^-}$.

Finally we consider neutralinos. The neutralino mass matrix is given by

$$-\mathcal{L}_m = \frac{1}{2} \left(\tilde{B}_L \tilde{W}_L^0 \tilde{H}_{1L}^0 \tilde{H}_{2L}^0 \right) M_N \begin{pmatrix} \tilde{B}_L \\ \tilde{W}_L^0 \\ \tilde{H}_{1L}^0 \\ \tilde{H}_{2L}^0 \end{pmatrix} + h.c., \quad (70)$$

where

$$M_N = \begin{pmatrix} M_1 & 0 & -m_Z s_W c_\beta & m_Z s_W s_\beta \\ 0 & M_2 & m_Z c_W c_\beta & -m_Z c_W s_\beta \\ -m_Z s_W c_\beta & m_Z c_W c_\beta & 0 & -\mu \\ m_Z s_W s_\beta & -m_Z c_W s_\beta & -\mu & 0 \end{pmatrix}. \quad (71)$$

The diagonalization is done by a real orthogonal matrix O_N ,

$$O_N M_N O_N^\top = (\text{diagonal}). \quad (72)$$

The mass eigenstates are given by

$$\tilde{\chi}_{AL}^0 = (O_N)_{AB} \tilde{X}_{BL}^0, \quad (A, B = 1, \dots, 4), \quad (73)$$

where

$$\tilde{X}_{AL}^0 = (\tilde{B}_L, \tilde{W}_L^0, \tilde{H}_{1L}^0, \tilde{H}_{2L}^0). \quad (74)$$

We have thus Majorana spinors

$$\tilde{\chi}_A^0 = \tilde{\chi}_{AL}^0 + \tilde{\chi}_{AR}^0, \quad (75)$$

with the mass $M_{\tilde{\chi}_A^0}$.

We now give the interaction Lagrangian of the SUSY particles. First, the fermion-sfermion-chargino interaction is given as

$$\begin{aligned}\mathcal{L}_{\text{int}} = & -g_2 \overline{\tilde{\chi}_A^-} (C_{iAX}^{R(l)} P_R + C_{iAX}^{L(l)} P_L) l_i \tilde{\nu}_X^\dagger \\ & -g_2 \overline{\tilde{\chi}_A^+} (C_{iAX}^{R(\nu)} P_R + C_{iAX}^{L(\nu)} P_L) \nu_i \tilde{l}_X^\dagger \\ & -g_2 \overline{\tilde{\chi}_A^-} (C_{iAX}^{R(d)} P_R + C_{iAX}^{L(d)} P_L) d_i \tilde{u}_X^\dagger \\ & -g_2 \overline{\tilde{\chi}_A^+} (C_{iAX}^{R(u)} P_R + C_{iAX}^{L(u)} P_L) u_i \tilde{d}_X^\dagger + h.c.,\end{aligned}\quad (76)$$

where the coefficients are

$$\begin{aligned}C_{iAX}^{L(l)} &= (O_R)_{A1} U_{X,i}^\nu, \\ C_{iAX}^{R(l)} &= -\frac{m_{l_i}}{\sqrt{2} m_W c_\beta} (O_L)_{A2} U_{X,i}^\nu, \\ C_{iAX}^{L(\nu)} &= \{(O_L)_{A1} U_{X,i}^l - \frac{m_{l_i}}{\sqrt{2} m_W c_\beta} (O_L)_{A2} U_{X,i+3}^l\}, \\ C_{iAX}^{R(\nu)} &= 0, \\ C_{iAX}^{L(d)} &= \{(O_R)_{A1} U_{X,i}^u - \frac{m_{u_i}}{\sqrt{2} m_W s_\beta} (O_R)_{A2} U_{X,i+3}^u\}, \\ C_{iAX}^{R(d)} &= -\frac{m_{d_i}}{\sqrt{2} m_W c_\beta} (O_L)_{A2} U_{X,i}^u, \\ C_{iAX}^{L(u)} &= \{(O_L)_{A1} U_{X,i}^d - \frac{m_{d_i}}{\sqrt{2} m_W c_\beta} (O_L)_{A2} U_{X,i+3}^d\}, \\ C_{iAX}^{R(u)} &= -\frac{m_{u_i}}{\sqrt{2} m_W s_\beta} (O_R)_{A2} U_{X,i}^d.\end{aligned}\quad (77)$$

The interaction Lagrangian of fermion-sfermion-neutralino is similarly written as

$$\mathcal{L}_{\text{int}} = -g_2 \overline{\tilde{\chi}_A^0} (N_{iAX}^{R(f)} P_R + N_{iAX}^{L(f)} P_L) f_i \tilde{f}_X^\dagger + h.c., \quad (78)$$

where f stands for l, ν, d , and u . The coefficients are

$$\begin{aligned}N_{iAX}^{L(l)} &= \frac{1}{\sqrt{2}} \{[-(O_N)_{A2} - (O_N)_{A1} t_W] U_{X,i}^l + \frac{m_{l_i}}{m_W c_\beta} (O_N)_{A3} U_{X,i+3}^l\}, \\ N_{iAX}^{R(l)} &= \frac{1}{\sqrt{2}} \{\frac{m_{l_i}}{m_W c_\beta} (O_N)_{A3} U_{X,i}^l + 2(O_N)_{A1} t_W U_{X,i+3}^l\}, \\ N_{iAX}^{L(\nu)} &= \frac{1}{\sqrt{2}} [(O_N)_{A2} - (O_N)_{A1} t_W] U_{X,i}^\nu,\end{aligned}$$

$$\begin{aligned}
N_{iAX}^{R(\nu)} &= 0, \\
N_{iAX}^{L(d)} &= \frac{1}{\sqrt{2}} \{ [-(O_N)_{A2} + \frac{1}{3}(O_N)_{A1}t_W] U_{X,i}^d + \frac{m_{d_i}}{m_W c_\beta} (O_N)_{A3} U_{X,i+3}^d \}, \\
N_{iAX}^{R(d)} &= \frac{1}{\sqrt{2}} \{ \frac{m_{d_i}}{m_W c_\beta} (O_N)_{A3} U_{X,i}^d + \frac{2}{3} t_W (O_N)_{A1} U_{X,i+3}^d \}, \\
N_{iAX}^{L(u)} &= \frac{1}{\sqrt{2}} \{ [(O_N)_{A2} + \frac{1}{3}(O_N)_{A1}t_W] U_{X,i}^u + \frac{m_{u_i}}{m_W s_\beta} (O_N)_{A4} U_{X,i+3}^u \}, \\
N_{iAX}^{R(u)} &= \frac{1}{\sqrt{2}} \{ \frac{m_{u_i}}{m_W s_\beta} (O_N)_{A4} U_{X,i}^u - \frac{4}{3} t_W (O_N)_{A1} U_{X,i+3}^u \}.
\end{aligned} \tag{79}$$

Next, the interaction of sfermion- Z boson is presented as

$$\mathcal{L} = -ig_Z z_{XY}^{(\tilde{f})} \tilde{f}_X^\dagger \partial^\mu \tilde{f}_Y Z_\mu + h.c.,$$

where

$$z_{XY}^{(\tilde{f})} = T_{3L}^f \sum_{i=1}^3 U_{X,i}^f U_{Y,i}^f - Q s_W^2 \delta_{XY}, \tag{80}$$

and $g_Z^2 = g_2^2 + g_Y^2$. The interaction of chargino or neutralino to Z boson is given as

$$\begin{aligned}
\mathcal{L} = & -\frac{1}{2} g_Z z_{AB}^{(\tilde{\chi}^0)} \overline{\tilde{\chi}_A^0} \gamma^\mu P_L \tilde{\chi}_B^0 Z_\mu \\
& - g_Z z_{AB}^{(\tilde{\chi}^-)} \overline{\tilde{\chi}_A^-} \gamma^\mu \left(z_{LAB}^{(\tilde{\chi}^-)} P_L + z_{RAB}^{(\tilde{\chi}^-)} P_R \right) \tilde{\chi}_B^- Z_\mu,
\end{aligned} \tag{81}$$

where

$$\begin{aligned}
z_{AB}^{(\tilde{\chi}^0)} &= ((O_N)_{A3}(O_N)_{B3} - (O_N)_{A4}(O_N)_{B4}), \\
z_{LAB}^{(\tilde{\chi}^-)} &= \left(\frac{1}{2} (O_L)_{A2}(O_L)_{B2} - c_W^2 \delta_{AB} \right), \\
z_{RAB}^{(\tilde{\chi}^-)} &= \left(\frac{1}{2} (O_R)_{A2}(O_R)_{B2} - c_W^2 \delta_{AB} \right).
\end{aligned} \tag{82}$$

The interaction of chargino and neutralino to W boson is also

$$\mathcal{L} = -g_2 \overline{\tilde{\chi}_A^0} \gamma_\mu \left(w_{LAB}^{(\tilde{\chi})} P_L + w_{RAB}^{(\tilde{\chi})} P_R \right) \tilde{\chi}_B^- W_\mu^+ + h.c., \tag{83}$$

where

$$\begin{aligned}
w_{LAB}^{(\tilde{\chi})} &= \left((O_N)_{A2}(O_L)_{B1} + \frac{1}{\sqrt{2}} (O_N)_{A3}(O_L)_{B2} \right), \\
w_{RAB}^{(\tilde{\chi})} &= \left((O_N)_{A2}(O_R)_{B1} - \frac{1}{\sqrt{2}} (O_N)_{A4}(O_R)_{B2} \right).
\end{aligned} \tag{84}$$

C Matrix elements of the off-shell slepton production and decay processes

We present the matrix elements of the off-shell slepton production and decay processes at $l_i^+ l_i^-$ collisions. First, we discuss the charged slepton pair production process with the center mass energy \sqrt{s} . The kinematics for the process $(l_i^-(p) \ l_i^+(\bar{p}) \rightarrow \tilde{l}_X^-(k) \ \tilde{l}_Y^+(\bar{k}))$ is given as

$$\begin{aligned} p &= \frac{\sqrt{s}}{2}(1, 0, 0, 1), \\ \bar{p} &= \frac{\sqrt{s}}{2}(1, 0, 0, -1), \\ k &= \left(\frac{s + \Delta k^2}{2\sqrt{s}}, \frac{\sqrt{s}}{2}\beta_p s_\theta, 0, \frac{\sqrt{s}}{2}\beta_p c_\theta\right), \\ \bar{k} &= \left(\frac{s - \Delta k^2}{2\sqrt{s}}, -\frac{\sqrt{s}}{2}\beta_p s_\theta, 0, -\frac{\sqrt{s}}{2}\beta_p c_\theta\right), \end{aligned} \quad (85)$$

where

$$\begin{aligned} \Delta k^2 &= k^2 - \bar{k}^2, \\ \beta_p^2 &= \frac{1}{s^2}(s^2 - 2s(k^2 + \bar{k}^2) + (\Delta k^2)^2). \end{aligned}$$

The amplitudes $\mathcal{M}_{XY}^{(h\bar{h})}$ with the helicity of $l_i^-(l_i^+)$ being $h(\bar{h})$ are given as

$$\begin{aligned} \mathcal{M}_{XY}^{(+)}(k^2, \bar{k}^2) &= -s\beta_p s_\theta \left\{ \frac{e^2}{s} \delta_{XY} + \frac{g_Z^2}{s - m_Z^2} z_{XY}^{(\bar{l})} z_R^{(l)} + \sum_A \frac{1}{2} \frac{g_2^2}{t - M_{\tilde{\chi}_A^0}^2} N_{iAX}^{R(l)} N_{iAY}^{R(l)} \right\}, \\ \mathcal{M}_{XY}^{(-)}(k^2, \bar{k}^2) &= s\beta_p s_\theta \left\{ \frac{e^2}{s} \delta_{XY} + \frac{g_Z^2}{s - m_Z^2} z_{XY}^{(\bar{l})} z_L^{(l)} + \sum_A \frac{1}{2} \frac{g_2^2}{t - M_{\tilde{\chi}_A^0}^2} N_{iAX}^{L(l)} N_{iAY}^{L(l)} \right\}, \\ \mathcal{M}_{XY}^{(++)}(k^2, \bar{k}^2) &= -\sum_A \sqrt{s} \frac{g_2^2}{t - M_{\tilde{\chi}_A^0}^2} N_{iAX}^{R(l)} N_{iAY}^{L(l)} M_{\tilde{\chi}_A^0}, \\ \mathcal{M}_{XY}^{(--)}(k^2, \bar{k}^2) &= -\sum_A \sqrt{s} \frac{g_2^2}{t - M_{\tilde{\chi}_A^0}^2} N_{iAX}^{L(l)} N_{iAY}^{R(l)} M_{\tilde{\chi}_A^0}, \end{aligned}$$

where $z_L^{(l)}(z_R^{(l)}) = -1/2 + s_W^2(s_W^2)$ and $t = (\Delta k^2)^2/4s - s(1 + \beta_p^2 - 2\beta_p c_\theta)/4$. Form these amplitudes the cross section of the on-shell charged slepton pair production $(l_i^- \ l_i^+ \rightarrow \tilde{l}_X^- \ \tilde{l}_Y^+)$ is given as

$$\frac{d\sigma}{dc_\theta} = \frac{1}{2s} \frac{\beta_p}{16\pi} \sum_{h\bar{h}} \left| \mathcal{M}_{XY}^{(h\bar{h})}(m_{\tilde{l}_X}^2, m_{\tilde{l}_Y}^2) \right|^2, \quad (86)$$

where $\overline{\Sigma}_{h\bar{h}}$ means the average over the helicities of the initial beams. Similarly, the helicity amplitudes of off-shell sneutrino pair production ($l_i^-(p) l_i^+(\bar{p}) \rightarrow \tilde{\nu}_X(k) \tilde{\nu}_Y(\bar{k})$) are given as

$$\begin{aligned}\mathcal{M}_{XY}^{(+)}(k^2, \bar{k}^2) &= -s\beta_p s_\theta \left\{ \frac{g_Z^2}{s - m_Z^2} z_{XY}^{(\tilde{\nu})} z_R^{(l)} + \sum_A \frac{1}{2} \frac{g_2^2}{t - M_{\tilde{\chi}_A^-}^2} C_{iAX}^{R(l)} C_{iAY}^{R(l)} \right\}, \\ \mathcal{M}_{XY}^{(-)}(k^2, \bar{k}^2) &= s\beta_p s_\theta \left\{ \frac{g_Z^2}{s - m_Z^2} z_{XY}^{(\tilde{\nu})} z_L^{(l)} + \sum_A \frac{1}{2} \frac{g_2^2}{t - M_{\tilde{\chi}_A^-}^2} C_{iAX}^{L(l)} C_{iAY}^{L(l)} \right\}, \\ \mathcal{M}_{XY}^{(++)}(k^2, \bar{k}^2) &= -\sum_A \sqrt{s} \frac{g_2^2}{t - M_{\tilde{\chi}_A^-}^2} C_{iAX}^{R(l)} C_{iAY}^{L(l)} M_{\tilde{\chi}_A^-}, \\ \mathcal{M}_{XY}^{(--)}(k^2, \bar{k}^2) &= -\sum_A \sqrt{s} \frac{g_2^2}{t - M_{\tilde{\chi}_A^-}^2} C_{iAX}^{L(l)} C_{iAY}^{R(l)} M_{\tilde{\chi}_A^-}.\end{aligned}$$

Next, we show the matrix elements for the decay processes of the off-shell slepton. Now we assume that sleptons decay to two-body states. Those for $\tilde{l}_X^- \rightarrow \tilde{\chi}_A^- \nu_i$ (\mathcal{M}_{XAi}) are

$$\mathcal{M}_{XAi}(k^2) = g_2 C_{iAX}^{L(\nu)} \sqrt{k^2 \beta_d}, \quad (87)$$

where k^2 is square of the momentum of the slepton and $\beta_d = 1 - M_{\tilde{\chi}_A^-}^2/k^2$. We ignore the lepton mass. The partial decay width of the on-shell slepton is

$$\Gamma = \frac{1}{16\pi m_{\tilde{l}_X}} \beta_d |\mathcal{M}_{XAi}(m_{\tilde{l}_X})|^2. \quad (88)$$

The matrix elements for $\tilde{l}_X \rightarrow \tilde{\chi}_A^0 l_i$ with the helicity of l_i being h ($\mathcal{M}_{XAi}^{(h)}$) are

$$\begin{aligned}\mathcal{M}_{XAi}^{(+)}(k^2) &= g_2 N_{iAX}^{R(l)} \sqrt{k^2 \beta_d}, \\ \mathcal{M}_{XAi}^{(-)}(k^2) &= g_2 N_{iAX}^{L(l)} \sqrt{k^2 \beta_d}.\end{aligned} \quad (89)$$

Similarly, the matrix elements for $\tilde{\nu}_X \rightarrow \tilde{\chi}_A^+ l_i$ with the helicity of l_i being h ($\mathcal{M}_{XAi}^{(h)}$) are

$$\begin{aligned}\mathcal{M}_{XAi}^{(+)}(k^2) &= g_2 C_{iAX}^{R(l)} \sqrt{k^2 \beta_d}, \\ \mathcal{M}_{XAi}^{(-)}(k^2) &= g_2 C_{iAX}^{L(l)} \sqrt{k^2 \beta_d},\end{aligned} \quad (90)$$

and those for $\tilde{\nu}_X \rightarrow \tilde{\chi}_A^0 \nu_i$ are

$$\mathcal{M}_{XAi}(k^2) = g_2 N_{iAX}^{L(\nu)} \sqrt{k^2 \beta_d}. \quad (91)$$

D Partial decay widths for charginos and neutralinos

In this Appendix, we present the partial decay widths of charginos and neutralinos to three-body states. The partial decay width of chargino into neutralino is

$$\Gamma(\tilde{\chi}_A^- \rightarrow \tilde{\chi}_B^0 \tilde{f}_{\uparrow i} f_{\downarrow j}) = N_C \frac{1}{256\pi^3} |\mathcal{M}|^2 M_{\tilde{\chi}_A^-} dx dy, \quad (92)$$

where N_C is a color factor ($N_C = 3$ for $(\tilde{f}_{\uparrow i}, f_{\downarrow j}) = (\bar{u}, d)$ and $N_C = 1$ for $(\tilde{f}_{\uparrow i}, f_{\downarrow j}) = (\bar{\nu}, l)$).

The squared amplitude is

$$\begin{aligned} |\mathcal{M}|^2 = & 2A_L^2(1-y)(y-r_{\tilde{\chi}_B}^2) + 2A_R^2(1-x)(x-r_{\tilde{\chi}_B}^2) \\ & - 4A_L A_R r_{\tilde{\chi}_B} z, \end{aligned} \quad (93)$$

and the coefficients are given as

$$\begin{aligned} A_L &= \frac{g_2^2}{\sqrt{2}} \left\{ \frac{w_{LBA}^{(\tilde{\chi})}}{z-r_W^2} - \sum_X \frac{1}{\sqrt{2}} \frac{C_{iAX}^{L(f_{\uparrow})} N_{jBX}^{L(f_{\downarrow})}}{y-r_{\tilde{f}_{\uparrow X}}^2} \right\}, \\ A_R &= \frac{g_2^2}{\sqrt{2}} \left\{ \frac{w_{RBA}^{(\tilde{\chi})}}{z-r_W^2} + \sum_X \frac{1}{\sqrt{2}} \frac{C_{jAX}^{L(f_{\downarrow})} N_{iBX}^{L(f_{\uparrow})}}{x-r_{\tilde{f}_{\uparrow X}}^2} \right\}. \end{aligned}$$

Here, we ignore the Yukawa interaction of Higgsinos. The mass ratios $r_{\tilde{\chi}_B}$, r_W , $r_{\tilde{f}_{\uparrow X}}$, and $r_{\tilde{f}_{\downarrow X}}$ are defined as

$$\begin{aligned} r_{\tilde{\chi}_B} &= \frac{M_{\tilde{\chi}_B^0}}{M_{\tilde{\chi}_A^-}}, & r_W &= \frac{m_W}{M_{\tilde{\chi}_A^-}}, \\ r_{\tilde{f}_{\uparrow X}} &= \frac{m_{\tilde{f}_{\uparrow X}}}{M_{\tilde{\chi}_A^-}}, & r_{\tilde{f}_{\downarrow X}} &= \frac{m_{\tilde{f}_{\downarrow X}}}{M_{\tilde{\chi}_A^-}}. \end{aligned}$$

The boundary condition of the phase space is given as

$$\begin{aligned} z(xy - r_{\tilde{\chi}_B}^2) &\geq 0, \\ r_{\tilde{\chi}_B}^2 \leq x, y &\leq 1, \end{aligned} \quad (94)$$

and $x + y + z = 1 + r_{\tilde{\chi}_B}^2$.

The partial decay width of neutralino into the lighter neutralino is given as

$$\Gamma(\tilde{\chi}_A^0 \rightarrow \tilde{\chi}_B^0 \tilde{f}_i f_j) = N_C \frac{1}{256\pi^3} |\mathcal{M}|^2 M_{\tilde{\chi}_A^0} dx dy, \quad (95)$$

The squared amplitude is

$$|\mathcal{M}|^2 = 2(A_{LL}^2 + A_{RR}^2)(1-y)(y - r_{\tilde{\chi}_B}^2) + 2(A_{LR}^2 + A_{RL}^2)(1-x)(x - r_{\tilde{\chi}_B}^2) - 4(A_{LL}A_{RL} + A_{RR}A_{LR})r_{\tilde{\chi}_B}z, \quad (96)$$

and the coefficients are given as

$$\begin{aligned} A_{LL} &= \frac{1}{2}g_Z^2 \frac{z_{BA}^{(\tilde{\chi}_B^0)} z_L^{(f)}}{z - r_Z^2} - \sum_X \frac{1}{2}g_2^2 \frac{N_{jAX}^{L(f)} N_{iBX}^{L(f)}}{y - r_{\tilde{f}_X}^2}, \\ A_{RL} &= -\frac{1}{2}g_Z^2 \frac{z_{BA}^{(\tilde{\chi}_B^0)} z_L^{(f)}}{z - r_Z^2} + \sum_X \frac{1}{2}g_2^2 \frac{N_{iAX}^{L(f)} N_{jBX}^{L(f)}}{x - r_{\tilde{f}_X}^2}, \\ A_{LR} &= \frac{1}{2}g_Z^2 \frac{z_{BA}^{(\tilde{\chi}_B^0)} z_R^{(f)}}{z - r_Z^2} + \sum_X \frac{1}{2}g_2^2 \frac{N_{iAX}^{R(f)} N_{jBX}^{R(f)}}{x - r_{\tilde{f}_X}^2}, \\ A_{RR} &= -\frac{1}{2}g_Z^2 \frac{z_{BA}^{(\tilde{\chi}_B^0)} z_R^{(f)}}{z - r_Z^2} - \sum_X \frac{1}{2}g_2^2 \frac{N_{jAX}^{R(f)} N_{iBX}^{R(f)}}{y - r_{\tilde{f}_X}^2}, \end{aligned}$$

where $z_L^{(f)}(z_R^{(f)}) = T_{3L} - Qs_W^2(-Qs_W^2)$. Here, we also ignore the Yukawa interaction. The mass ratios $r_{\tilde{\chi}_B}$, r_Z , and $r_{\tilde{f}_X}$ are defined as

$$r_{\tilde{\chi}_B} = \frac{M_{\tilde{\chi}_B^0}}{M_{\tilde{\chi}_A^0}}, \quad r_Z = \frac{m_Z}{M_{\tilde{\chi}_A^-}}, \quad r_{\tilde{f}_X} = \frac{m_{\tilde{f}_X}}{M_{\tilde{\chi}_A^-}}.$$

The boundary condition of the phase space is the same as that in Eq. (94).

E Energy and IP distribution of muon from tau decay in flight

In this Appendix we present the energy and the IP distribution of muon from decay tau leptons in flight with the fixed energy E_τ . Here, we define σ_{IP} as distance between the interaction point where the tau lepton is produced and the track of muon.

First, we show the angular distribution of muon from tau lepton in flight. The momentum of tau lepton is given as $E_\tau(1, 0, 0, 1)$, and that of muon is $E_\mu(1, s_\theta c_\phi, s_\theta s_\phi, c_\theta)$. In this basis, the angular distribution is

$$\frac{d\Gamma}{\Gamma} = \rho(\gamma_\tau \theta, z) dz d(\gamma_\tau \theta), \quad (97)$$

where $z = E_\mu/E_\tau$, $\gamma_\tau = E_\tau/m_\tau$. The distribution function $\rho(y, z)$ is

$$\rho(y, z) = 4z^2y \left(3(1+y^2) - 2z(1+y^2)^2 + P_\tau \left\{ (1-y^2) - 2z(1-y^4) \right\} \right) \quad (98)$$

where P_τ is the helicity of tau lepton. Here, we take a limit of $\gamma_\tau^{-1} \rightarrow 0$. The boundary condition is

$$\begin{aligned} 0 \leq (\gamma_\tau \theta)^2 &\leq 1/z - 1, \\ 0 \leq z &\leq 1. \end{aligned} \quad (99)$$

By integrating θ , the energy distribution of muon from decay of tau lepton in flight is given as

$$\frac{d\Gamma}{\Gamma} = \frac{1}{3}(1-z)(5+5z-4z^2+P_\tau(1+z-8z^2))dz. \quad (100)$$

Since σ_{IP} is defined as distance between the interaction point and the track of muon, the IP parameter is

$$\sigma_{IP} \equiv \beta_\tau \gamma_\tau cts\theta \simeq c(\gamma_\tau \theta)t, \quad (101)$$

where t is time between production and decay of τ and $\beta_\tau^2 = 1/(1-\gamma_\tau^2)$. Then, the energy and the IP distribution is

$$\begin{aligned} \frac{d\Gamma}{\Gamma} &= \int_0^\infty \frac{dt}{\tau_\tau} e^{-\frac{t}{\tau_\tau}} \rho\left(\frac{\sigma_{IP}}{ct}, z\right) \frac{d\sigma_{IP}}{ct} dz \\ &= \left(\sum_{n=1}^6 A_n \left(\frac{\sigma_{IP}}{c\tau_\tau} \right)^n \right) \frac{d\sigma_{IP}}{\sigma_{IP}} dz, \end{aligned} \quad (102)$$

where

$$\begin{aligned} A_1 &= \sqrt{1/z-1} \left(\frac{12}{5}z + \frac{88}{15}z^2 - \frac{64}{15}z^3 + P_\tau \left(\frac{4}{15}z + \frac{32}{15}z^2 - \frac{32}{5}z^3 \right) \right) e^{-\frac{\sigma_{IP}}{\tau_\tau \sqrt{1/z-1}}}, \\ A_2 &= \left(-\frac{8}{5}z + \frac{58}{15}z^2 - \frac{34}{15}z^3 + P_\tau \left(\frac{4}{15}z + \frac{2}{15}z^2 - \frac{2}{5}z^3 \right) \right) e^{-\frac{\sigma_{IP}}{\tau_\tau \sqrt{1/z-1}}} \\ &\quad + \left(12z^2 - 8z^3 + P_\tau(4z^2 - 8z^3) \right) \text{Ei}\left(-\frac{\sigma_{IP}}{\tau_\tau \sqrt{1/z-1}}\right), \\ A_3 &= \sqrt{1/z-1} \left(\frac{28}{15}z^2 - \frac{38}{15}z^3 + P_\tau \left(-\frac{8}{15}z^2 - \frac{2}{15}z^3 \right) \right) e^{-\frac{\sigma_{IP}}{\tau_\tau \sqrt{1/z-1}}}, \\ A_4 &= \left(\frac{1}{15}z^2 - \frac{1}{15}z^3 + P_\tau \left(-\frac{1}{15}z^2 + \frac{1}{15}z^3 \right) \right) e^{-\frac{\sigma_{IP}}{\tau_\tau \sqrt{1/z-1}}} \\ &\quad + \left(2z^2 - \frac{8}{3}z^3 - \frac{2}{3}P_\tau z^2 \right) \text{Ei}\left(-\frac{\sigma_{IP}}{\tau_\tau \sqrt{1/z-1}}\right), \end{aligned}$$

$$\begin{aligned}
A_5 &= \sqrt{1/z - 1} \left(-\frac{1}{15} z^3 + P_\tau \frac{1}{15} z^3 \right) e^{-\frac{\sigma_{IP}}{\tau_\tau \sqrt{1/z - 1}}}, \\
A_6 &= \left(-\frac{1}{15} z^3 + \frac{1}{15} P_\tau z^3 \right) \text{Ei}\left(-\frac{\sigma_{IP}}{\tau_\tau \sqrt{1/z - 1}}\right).
\end{aligned}$$

Here τ_τ is the life time of tau lepton, and $\text{Ei}(x)$ is Exponential Integral,

$$\text{Ei}(-x) = - \int_x^\infty \frac{1}{t} e^{-t} dt.$$

References

- [1] Super-Kamiokande Collaboration, BU-98-17 (hep-ex/9807003).
- [2] S.P. Mikheyev and A.Y. Smirnov, *Yad. Fiz.* **42** (1985) 1441 [*Sov. J. Nucl. Phys.* **42** (1985) 913]; *Nuovo Cim.* **C9** (1986) 17;
L. Wolfenstein, *Phys. Rev. D* **17** (1978) 2369.
- [3] CHOOZ Collaboration, *Phys. Lett. B* **420** (1998) 397.
- [4] T. Yanagida, in *Proceedings of the Workshop on Unified Theory and Baryon Number of the Universe*, eds. O. Sawada and A. Sugamoto (KEK, 1979) p.95;
M. Gell-Mann, P. Ramond, and R. Slansky, in *Supergravity*, eds. P. van Nieuwenhuizen and D. Freedman (North Holland, Amsterdam, 1979).
- [5] For review, H.P. Nilles, *Phys. Rep.* **110** (1984) 1.
- [6] L. Hall, V. Kostelecky, and S. Raby, *Nucl. Phys. B* **267** (1986) 415.
- [7] R. Barbieri and L. Hall, *Phys. Lett. B* **338** (1994) 212;
J. Hisano, T. Moroi, K. Tobe, and M. Yamaguchi, *Phys. Lett. B* **391** (1997) 341;
Erratum-ibid **B397**(1997)357;
J. Hisano, D. Nomura, Y. Okada, Y. Shimizu, and M. Tanaka, KEK-TH-575 (hep-ph/9805367);
J. Hisano, D. Nomura, and T. Yanagida, KEK-TH-548 (hep-ph/9711348);
Y. Okada, K. Okumura, and Y. Shimizu, KEK-TH-535 (hep-ph/9708446).
- [8] R. Barbieri, L. Hall, and A. Strumia, *Nucl. Phys. B* **445** (1995) 219,
P. Ciafaloni, A. Romanino, and A. Strumia, *Nucl. Phys. B* **458** (1996) 3;
N. Arkani-Hamed, H.-C. Cheng, and L.J. Hall, *Phys. Rev. D* **53** (1996) 413.
- [9] F. Gabbiani and A. Masiero, *Phys. Lett. B* **209** (1988) 289.
- [10] F. Borzumati and A. Masiero, *Phys. Rev. Lett.* **57** (1986) 961.
- [11] J. Hisano, T. Moroi, K. Tobe, M. Yamaguchi, and T. Yanagida, *Phys. Lett. B* **357** (1995) 579.
- [12] J. Hisano, T. Moroi, K. Tobe, and M. Yamaguchi, *Phys. Rev. D* **53** (1996) 2442.

- [13] N. Arkani-Hamed, H.-C. Cheng, J.L. Feng, and L.J. Hall, *Phys. Rev. Lett.* **77** (1996) 1937.
- [14] N. Arkani-Hamed, H.-C. Cheng, J.L. Feng, and L.J. Hall, *Nucl. Phys.* **B505** (1997) 7.
- [15] B. Baer, R. Munroe, and , X. Tata, *Phys. Rev.* **D54** (1996) 6735; *Erratum-ibid* **D56** (1997)4424.
- [16] N.V. Krasnikov, *Mod. Phys. Lett.* **A9** (1994) 791.
- [17] H.-C. Cheng, FERMILAB-CONF-97-418-T (hep-ph/9712427).
- [18] M. Hirouchi, and M. Tanaka, OU-HET-286 (hep-ph/9712532).
- [19] T. Goto and Y. Okada, *Prog. Theor. Phys.* **94** (1995) 407.
- [20] A. Miyamoto in *Proceedings of the Workshop on Physics and Experiments with Linear Colliders*, eds. A. Miyamoto et al (1995) p.654.
- [21] M.M. Nojiri, K. Fujii, and T. Tsukamoto, *Phys. Rev.* **D54** (1996) 6756.
- [22] B.K. Bullock, K. Hagiwara, and A.D. Martin *Nucl. Phys.* **B395** (1993) 499.
- [23] M.M. Nojiri, *Phys. Rev.* **D51** (1995) 6281.
- [24] JLC Group, *JLC-1* (KEK-Report-92-16).
- [25] The NLC Accelerator Design Group and The NLC Physics Working Group, *Physics and Technology of the Next Linear Collider* (SLAC-Report-485).
- [26] T. Tsukamoto *et al*, *Phys. Rev.* **D51** (1995) 3153.

(GeV)	$\tan \beta = 3$	$\tan \beta = 10$
$m_{\tilde{\chi}_1^0}$	56	58
$m_{\tilde{\chi}_2^0}$	105	103
$m_{\tilde{\chi}_1^-}$	100	100
$m_{\tilde{\nu}_\mu}$	180	180
$m_{\tilde{\mu}_L}$	194	197
$m_{\tilde{\mu}_R}$	159	164
μ	244	200

Table 1: The sample SUSY parameters in our calculation. We fix the lightest chargino mass ($m_{\tilde{\chi}_1^-}$) 100 GeV and the muon sneutrino mass ($m_{\tilde{\nu}_\mu}$) 180 GeV. The lightest and the second-lightest neutralino masses ($m_{\tilde{\chi}_1^0}$, $m_{\tilde{\chi}_2^0}$), the left-handed and the right-handed smuon masses ($m_{\tilde{\mu}_L}$, $m_{\tilde{\mu}_R}$), and other SUSY parameters are calculated by solving the RG equations, assuming the minimal supergravity scenario and the GUT relation for the gaugino masses. Here, the Higgsino mass parameter μ is determined by the radiative electroweak symmetry breaking condition with $\mu > 0$.

	$\tan \beta = 3$	$\tan \beta = 10$
$\tilde{e}_L^+ \tilde{e}_L^-$	146	136
$\tilde{\mu}_L^+ \tilde{\mu}_L^- (\tilde{\tau}_L^+ \tilde{\tau}_L^-)$	30	26
$\tilde{\nu}_e \tilde{\nu}_e^c$	957	966
$\tilde{\nu}_\mu \tilde{\nu}_\mu^c (\tilde{\nu}_\tau \tilde{\nu}_\tau^c)$	18	18

Table 2: Cross sections in fb for the left-handed slepton production at the e^+e^- collider with $\sqrt{s} = 500$ GeV. We fix $m_{\tilde{\nu}_\mu} = 180$ GeV, $\Delta m_{\tilde{\nu}} = 1$ GeV and $\theta_{\tilde{\nu}} = 0$. The other SUSY parameters are the same as in Table (1).

	$\tan \beta = 3$	$\tan \beta = 10$
$Br(\tilde{\mu}_L^-(\tilde{e}_L^-) \rightarrow \mu^-(e^-)\tilde{\chi}_1^0)$	0.05	0.08
$Br(\tilde{\mu}_L^-(\tilde{e}_L^-) \rightarrow \mu^-(e^-)\tilde{\chi}_2^0)$	0.39	0.41
$Br(\tilde{\mu}_L^-(\tilde{e}_L^-) \rightarrow \nu_\mu(\nu_e)\tilde{\chi}_1^-)$	0.56	0.51
$Br(\tilde{\tau}_L^- \rightarrow \tau^-\tilde{\chi}_1^0)$	0.06	0.12
$Br(\tilde{\tau}_L^- \rightarrow \tau^-\tilde{\chi}_2^0)$	0.38	0.38
$Br(\tilde{\tau}_L^- \rightarrow \nu_\tau\tilde{\chi}_1^-)$	0.56	0.50
$Br(\tilde{\nu}_\mu(\tilde{\nu}_e) \rightarrow \nu_\mu(\nu_e)\tilde{\chi}_1^0)$	0.30	0.26
$Br(\tilde{\nu}_\mu(\tilde{\nu}_e) \rightarrow \nu_\mu(\nu_e)\tilde{\chi}_2^0)$	0.14	0.15
$Br(\tilde{\nu}_\mu(\tilde{\nu}_e) \rightarrow \mu^-(e^-)\tilde{\chi}_1^+)$	0.56	0.59
$Br(\tilde{\nu}_\tau \rightarrow \nu_\tau\tilde{\chi}_1^0)$	0.30	0.26
$Br(\tilde{\nu}_\tau \rightarrow \nu_\tau\tilde{\chi}_2^0)$	0.14	0.15
$Br(\tilde{\nu}_\tau \rightarrow \tau^-\tilde{\chi}_1^+)$	0.56	0.59

Table 3: Branching ratios for the left-handed slepton decays. The input parameters are the same as in Table (1).

	$\tan \beta = 3$	$\tan \beta = 10$
$Br(\tilde{\chi}_1^- \rightarrow 2jets\tilde{\chi}_1^0)$	0.63	0.65
$Br(\tilde{\chi}_1^- \rightarrow l^-\bar{\nu}_l\tilde{\chi}_1^0)$	$0.37 \div 3$	$0.35 \div 3$
$Br(\tilde{\chi}_2^0 \rightarrow 2jets\tilde{\chi}_1^0)$	0.23	0.49
$Br(\tilde{\chi}_2^0 \rightarrow l^-l^+\tilde{\chi}_1^0)$	$0.42 \div 3$	$0.28 \div 3$
$Br(\tilde{\chi}_2^0 \rightarrow \nu_l\bar{\nu}_l\tilde{\chi}_1^0)$	$0.35 \div 3$	$0.23 \div 3$

Table 4: Branching ratios of the lightest chargino and second-lightest neutralino three-body decays. The input parameters are the same as in Table (1).

	$\tan \beta = 3$	$\tan \beta = 10$
$\tilde{\mu}_L^+\tilde{\mu}_L^-$	146	136
$\tilde{\tau}_L^+\tilde{\tau}_L^- (\tilde{e}_L^+\tilde{e}_L^-)$	30	26
$\tilde{\nu}_\mu\tilde{\nu}_\mu^c$	957	966
$\tilde{\nu}_\tau\tilde{\nu}_\tau^c(\tilde{\nu}_e\tilde{\nu}_e^c)$	18	18

Table 5: Cross sections in fb for the left-handed slepton production at the $\mu^+\mu^-$ collider with $\sqrt{s} = 500$ GeV. The input parameters are the same as in Table (1).

σ_{IP}^{cut}	$10\mu m$	$30\mu m$	(∞)
p_μ	0.02	0.04	0.09
p_τ	0.88	0.82	0.64

Table 6: The tau identification probability p_τ and the the muon misidentification probability p_μ for the IP cut $\sigma_{IP}^{\text{cut}} = 10$ and $30\mu m$, and ∞ . The parameter set is the same as in Fig. (6).

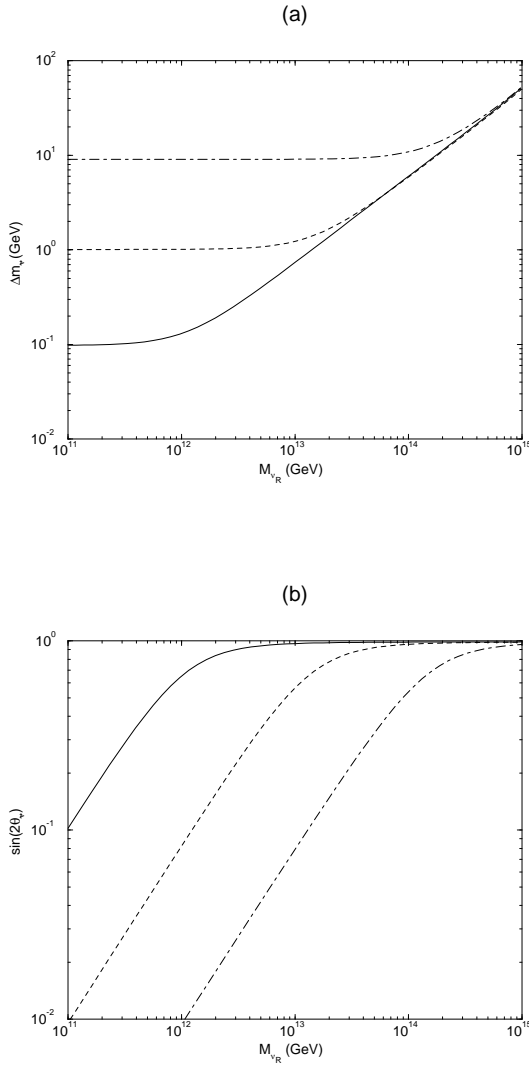


Figure 1: a) The mixing angle between the tau and muon sneutrinos ($\sin 2\theta_{\tilde{\nu}}$) and b) the mass difference ($\Delta m_{\tilde{\nu}}$) between the two non-e-like sneutrinos as a function of the right-handed neutrino scale. Here, we take $m_{\nu_\tau}^2 = 0.005 \text{ eV}^2$, $\theta_D = \pi/4$, and $\bar{m}_{\tilde{\nu}} = 180 \text{ GeV}$. For simplicity, the gaugino masses in the MSSM are given by the GUT relation, and the lightest chargino mass is taken to be 100GeV. The other parameters are determined in the minimal supergravity scenario and the radiative breaking condition of $SU(2)_L \times U(1)_Y$ with the Higgsino mass (μ) positive. Solid line, dashed line, and dash-dot line are for $\tan \beta = 3, 10$, and 30 .

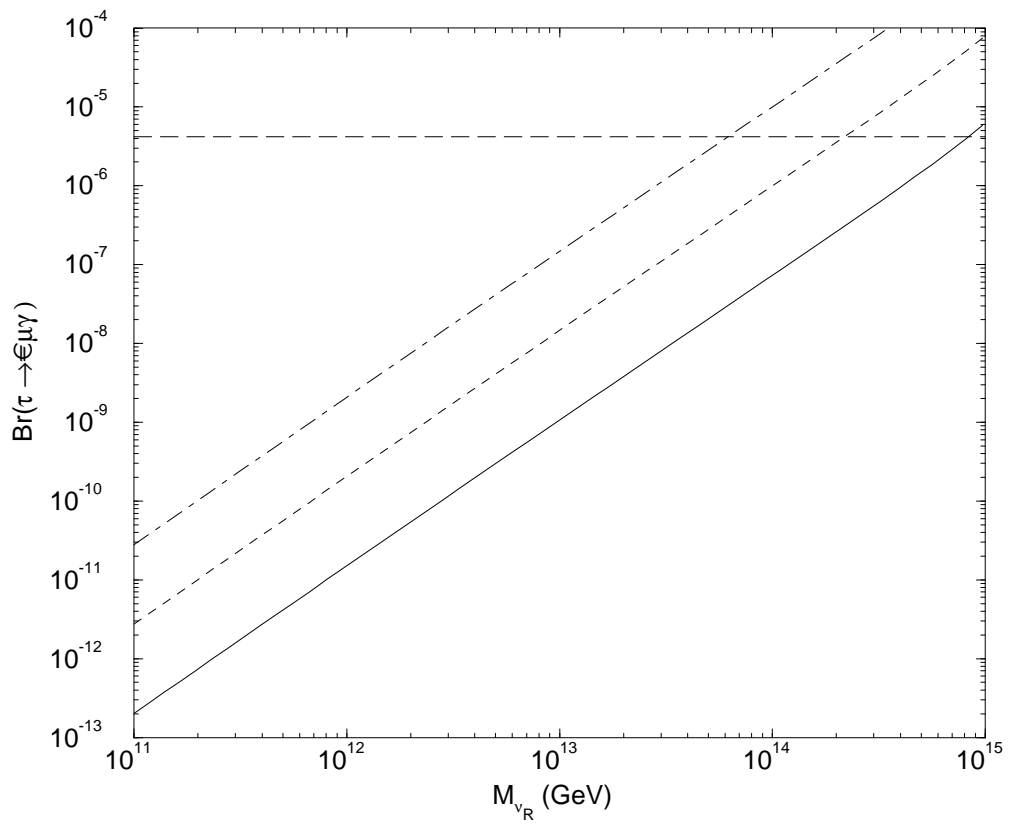


Figure 2: Branching ratio of $\tau \rightarrow \mu\gamma$ as a function of the right-handed neutrino scale. The input parameters are the same as in Fig. (1). The long-dashed line is the current experimental bound.

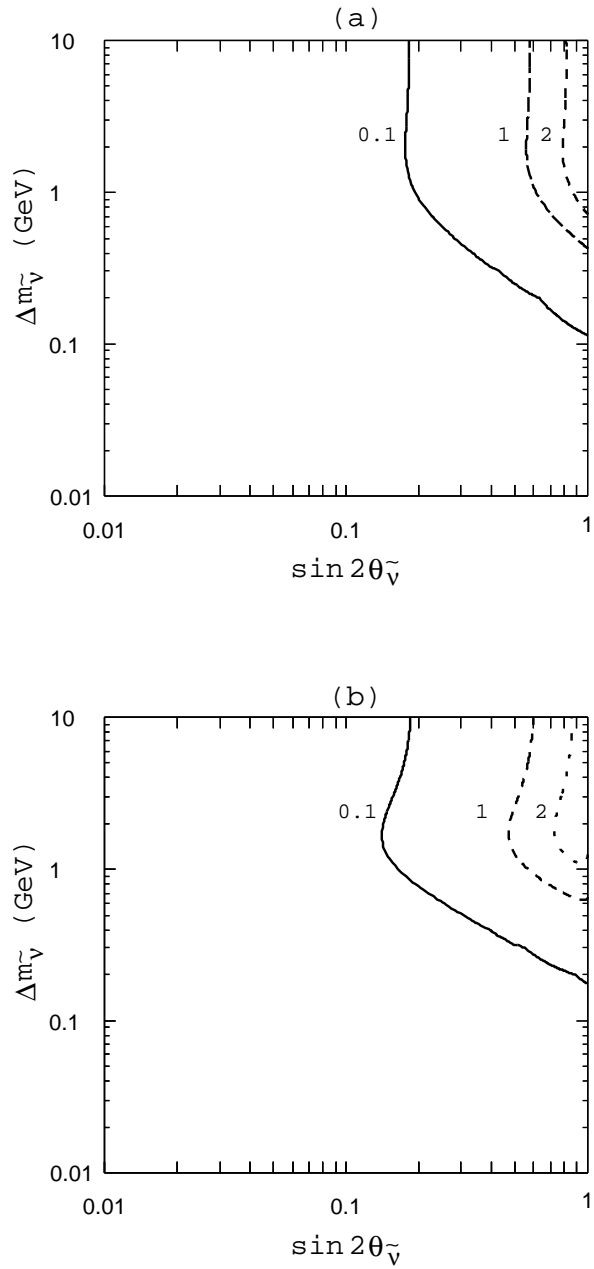


Figure 3: Cross sections of (a) $e^+e^- \rightarrow \tau^+\mu^- + \tilde{\chi}_1^-\tilde{\chi}_1^+$ and (b) $e^+e^- \rightarrow \tau^+\mu^- + \tilde{\chi}_2^0\tilde{\chi}_2^0$ at the center mass energy 500GeV. We show them as functions of $\Delta m_{\tilde{\nu}}$ and $\sin 2\theta_{\tilde{\nu}}$. Here, we take the sample SUSY parameter set for $\tan\beta = 3$ listed in Table (1).

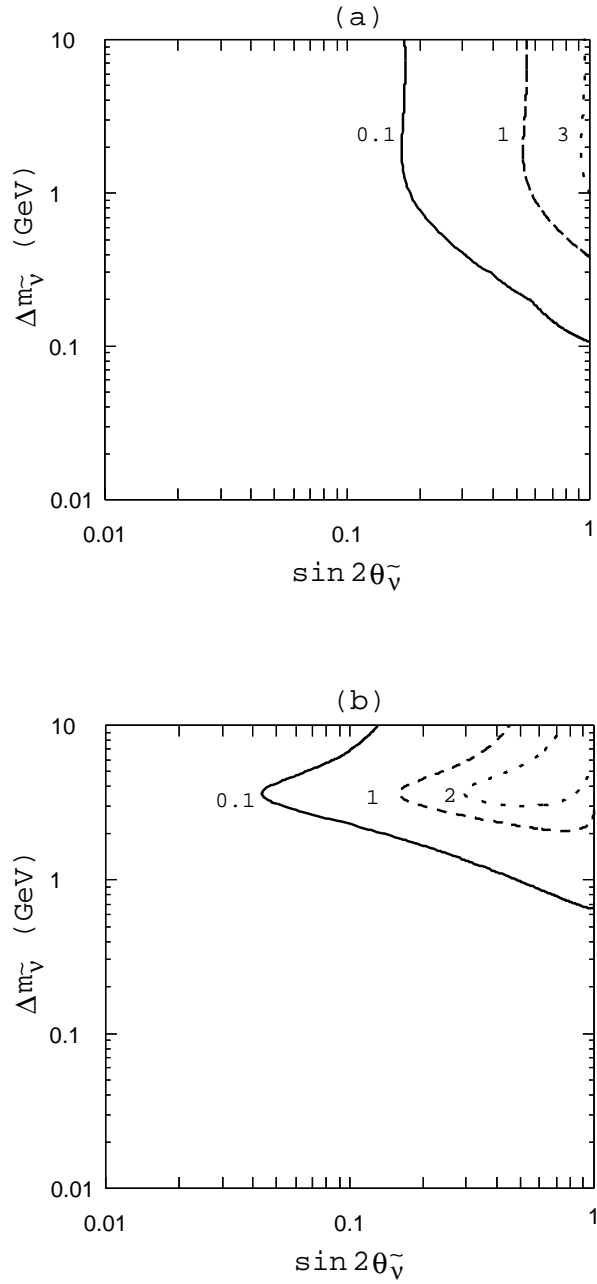


Figure 4: Cross sections of (a) $e^+e^- \rightarrow \tau^+\mu^- + \tilde{\chi}_1^-\tilde{\chi}_1^+$ and (b) $e^+e^- \rightarrow \tau^+\mu^- + \tilde{\chi}_2^0\tilde{\chi}_2^0$ at the center mass energy 500GeV. We show them as functions of $\Delta m_{\tilde{\nu}}$ and $\sin 2\theta_{\tilde{\nu}}$. Here, we take the SUSY sample parameter set for $\tan \beta = 10$ listed in Table (1).

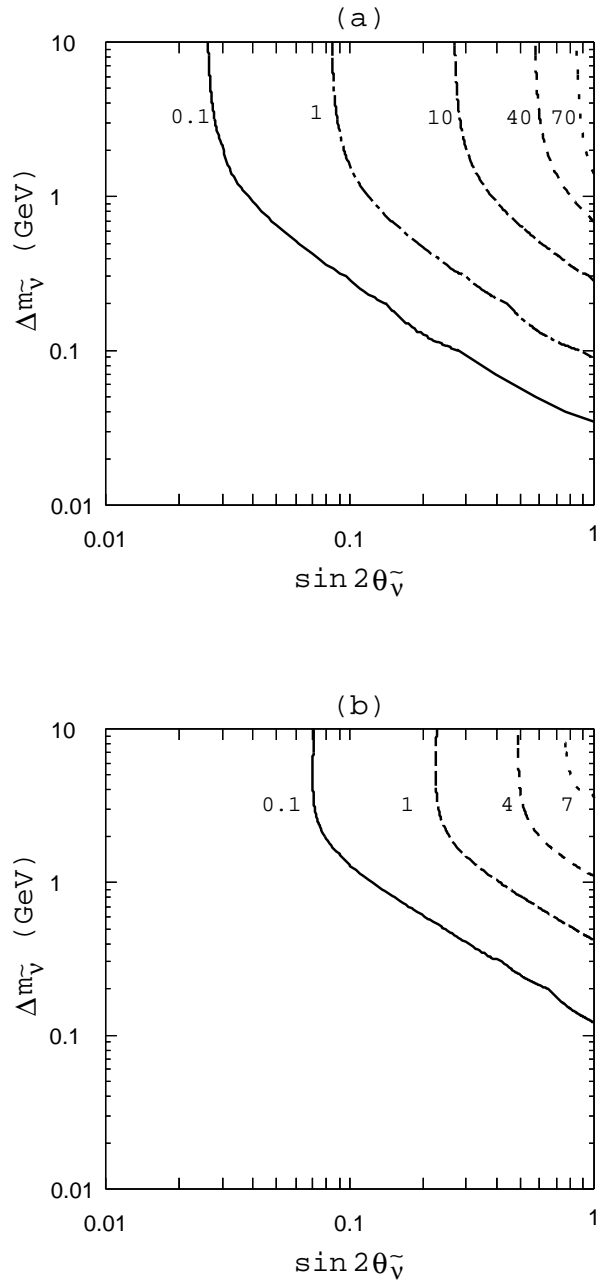


Figure 5: Cross sections of (a) $\mu^+ \mu^- \rightarrow \tau^+ \tau^- + \tilde{\chi}_1^- \tilde{\chi}_1^+$ and (b) $\mu^+ \mu^- \rightarrow \tau^+ \tau^- + \tilde{\chi}_2^0 \tilde{\chi}_2^0$ at the center mass energy 500GeV. We show them as functions of $\Delta m_{\tilde{\nu}}$ and $\sin 2\theta_{\tilde{\nu}}$. Here, we take the sample SUSY parameter set for $\tan \beta = 3$ listed in Table (1).

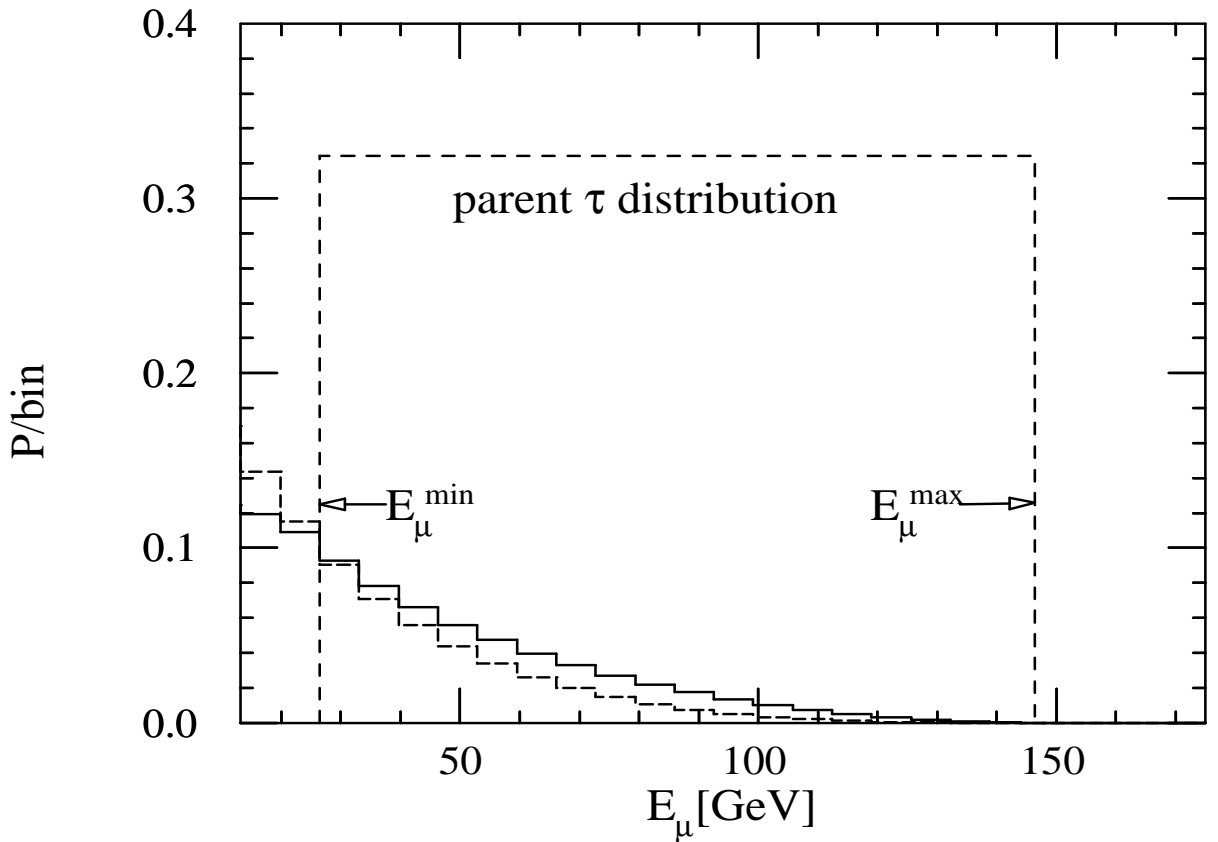


Figure 6: Energy distribution of μ from decaying τ in flight. The τ comes from the sneutrino pair production and the decay to chargino with the center mass energy 500GeV. Here, we take the sneutrino mass 180GeV, the chargino mass 100GeV. The energy distribution of the τ is flat between E_μ^{\min} and E_μ^{\max} . The solid and dashed lines are the energy distributions of μ from decaying τ with polarization -1 and $+1$, respectively.

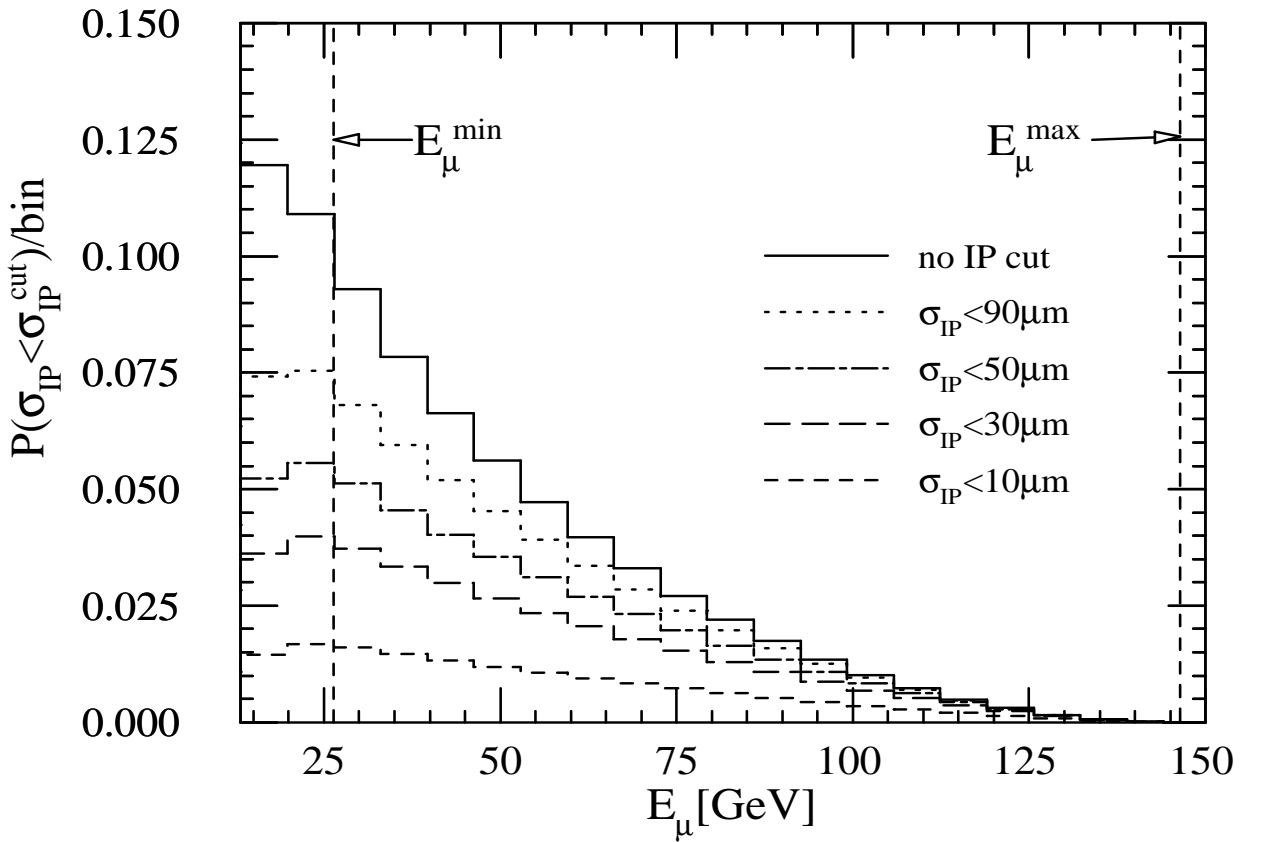


Figure 7: Energy distribution of μ from decaying τ , surviving after requiring the IP cut $\sigma_{IP} < \sigma_{IP}^{cut} = 10, 30, 50, 90 \mu m$. The τ comes from the slepton decay. The input parameter set is the same as in Fig. (6).

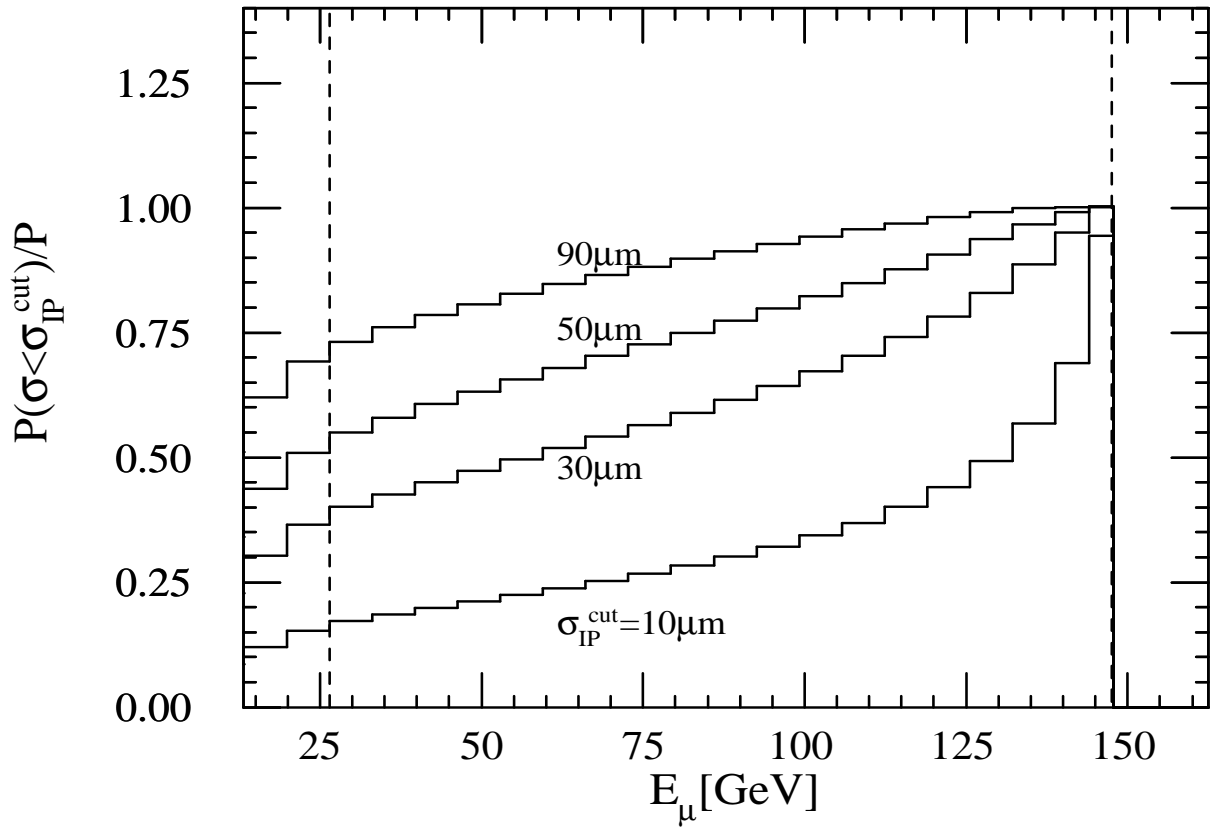


Figure 8: Energy distribution of μ from decaying τ after the IP cut $\sigma_{IP} < \sigma_{IP}^{cut}$ as the ratio to E_μ distribution without σ_{IP} cut. The input parameter set is the same as in Fig. (6).

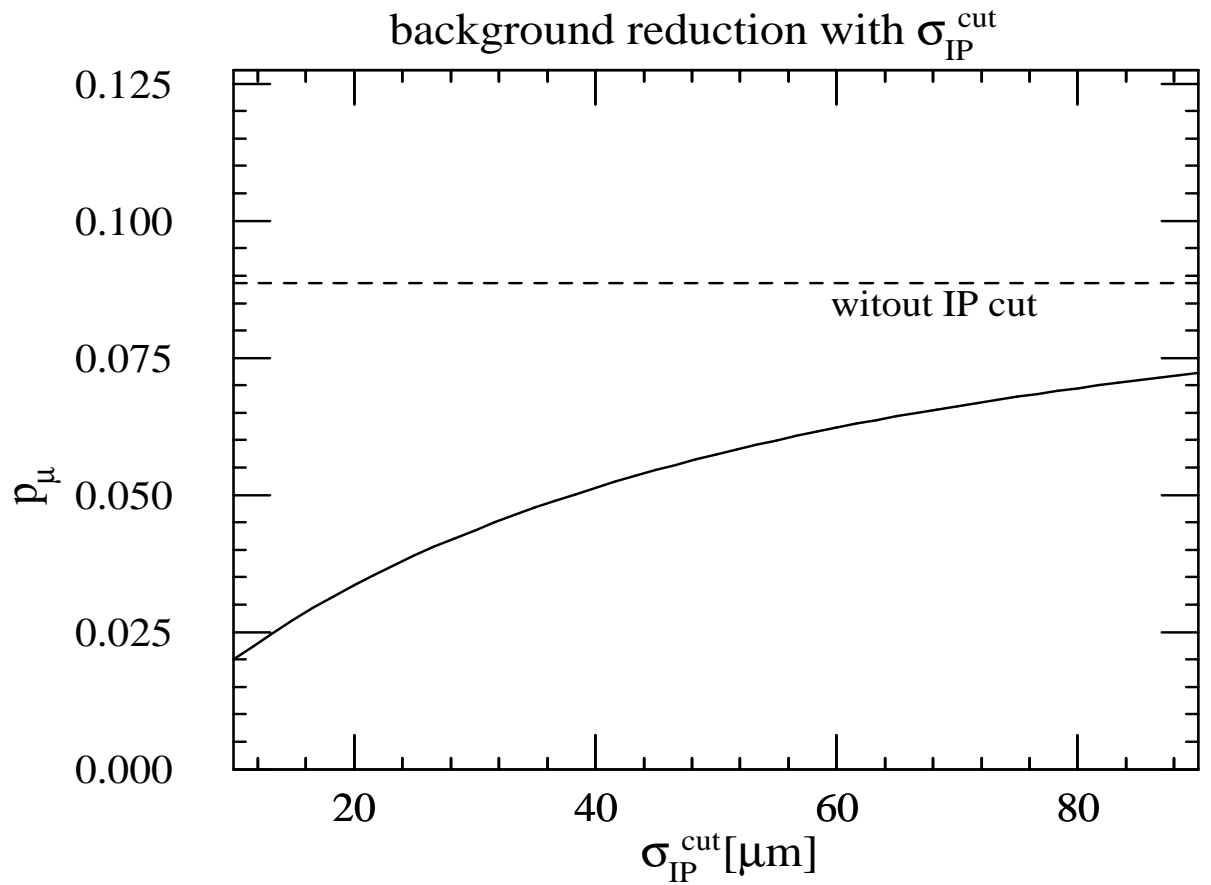


Figure 9: Probability p_μ that $\tilde{\nu}$ production and its decay into τ is mis-identified as $\tilde{\nu} \rightarrow \mu \tilde{\chi}$ when some σ_{IP}^{cut} are applied in addition to the energy cut $E_\mu > E_\mu^{\min}$. The parameter set is the same as in Fig. (6).

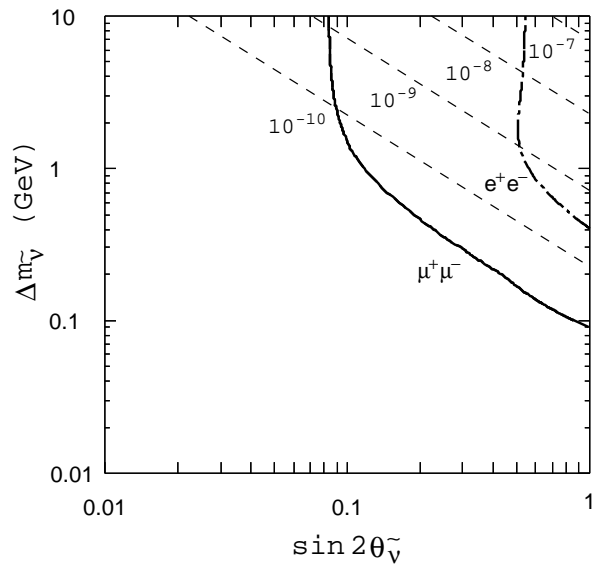


Figure 10: Significance contours corresponding to 3σ discovery as functions of $\sin 2\theta_{\tilde{\nu}}$ and $\Delta m_{\tilde{\nu}}$. The dashed-dot (solid) line is for a e^+e^- ($\mu^+\mu^-$) collider with the center mass energy 500GeV. We assume integrated luminosity $\mathcal{L} = 50\text{fb}^{-1}$. For the e^+e^- collider we take $\sigma_{IP}^{\text{cut}} = 10\mu\text{m}$. Here, we take the sample SUSY parameter set for $\tan\beta = 3$ listed in Table (1). We also show contours of the constant branching ratio of $\tau \rightarrow \mu\gamma$, 10^{-7} , 10^{-8} , 10^{-9} , and 10^{-10} by the dashed lines.